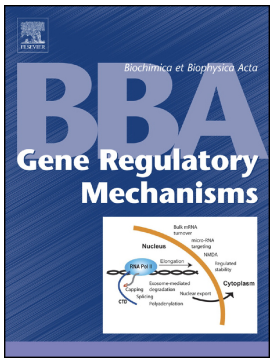

Functional validation of miRNAs targeting genes of DNA double-strand break repair to radiosensitize non-small lung cancer cells

Celeste Piotto, Alberto Biscontin, Caterina Millino, Maddalena Mognato

PII: S1874-9399(18)30111-1
DOI: https://doi.org/10.1016/j.bbagrm.2018.10.010
Reference: BBAGRM 94324

To appear in: *BBA - Gene Regulatory Mechanisms*

Received date: 22 March 2018
Revised date: 18 October 2018
Accepted date: 23 October 2018

Please cite this article as: Celeste Piotto, Alberto Biscontin, Caterina Millino, Maddalena Mognato , Functional validation of miRNAs targeting genes of DNA double-strand break repair to radiosensitize non-small lung cancer cells. Bbagrm (2018), https://doi.org/10.1016/j.bbagrm.2018.10.010

Functional validation of miRNAs targeting genes of DNA double-strand break repair to radiosensitize non-small lung cancer cells

Celeste Piotto[a], Alberto Biscontin[a], Caterina Millino[b], Maddalena Mognato[a*]

[a]Department of Biology, School of Sciences, University of Padova, via U. Bassi 58 B, 35131 Padova, Italy

[b]CRIBI Biotechnology Centre, University of Padova, via U. Bassi 58/B, 35131 Padova, Italy,

*****Correspondence: maddalena.mognato@unipd.it; Tel.: +39-049-8276274; Fax +39-049-8276280

Abstract

DNA-Double strand breaks (DSBs) generated by radiation therapy represent the most efficient lesions to kill tumor cells, however, the inherent DSB repair efficiency of tumor cells can cause cellular radioresistance and impact on therapeutic outcome. Genes of DSB repair represent a target for cancer therapy since their down-regulation can impair the repair process making the cells more sensitive to radiation. In this study, we analyzed the combination of ionizing radiation (IR) along with microRNA-mediated targeting of genes involved in DSB repair to sensitize human non-small cell lung cancer (NSCLC) cells. MicroRNAs are natural occurring modulators of gene expression and therefore represent an attractive strategy to affect the expression of DSB repair genes. As possible IR-sensitizing targets genes we selected genes of homologous recombination (HR) and non-homologous end joining (NHEJ) pathway (i.e. *RAD51, BRCA2, PRKDC, XRCC5, LIG1*). We examined these genes to determine whether they may be real targets of selected miRNAs by functional and biological validation. The *in vivo* effectiveness of miRNA treatments has been examined in cells over-expressing miRNAs and treated with IR. Taken together, our results show that hsa-miR-96-5p and hsa-miR-874-3p can directly regulate the expression of target genes. When these miRNAs are combined with IR can decrease the survival of NSCLC cells to a higher extent than that exerted by radiation alone, and similarly to radiation combined with specific chemical inhibitors of HR and NHEJ repair pathway.

Introduction

DNA damage caused by ionizing radiation (IR) during radiotherapy consists in a variety of DNA lesions, among which double-strand breaks (DSBs) represent the major lethal ones responsible for the cell killing of tumor cells. In response to DSBs eukaryotic cells activate the DNA-Damage Response (DDR), a complex pathway addressed to maintain genome integrity through the activation of proteins involved in sensing, signaling, and transducing the DNA damage signal to effector proteins of cell cycle progression/arrest, DNA repair and apoptosis [1]. In mammalian cells, the MRE11, RAD50, NBS1 (MRN) complex binds to the DNA surrounding the lesion, resects the DNA around the DSB break in a 5'–3' dependent direction, promoting appropriate repair by two evolutionarily primary mechanisms: homologous recombination (HR) and non-homologous end joining (NHEJ). HR predominates in the mid-S and mid-G2 cell cycle phases, when the sister template is available [2]. Replication Protein A (RPA) recognizes and binds the 3′ ends, then it is displaced by BRCA2, allowing binding of RAD51 and initiation of repair by HR. RAD51 loading at sites of DNA damage requires many factors, including BRCA1, BRCA2/ FANCD1, PALB2/FANCN and the RAD51 paralogs (RAD51B, RAD51C/FANCO, RAD51D, XRCC2, and XRCC3), and catalyzes the strand capture and invasion of broken ends of DSBs into intact homologous DNA sequences to ensure the fidelity of the repair process [3]. In addition to HR, DSBs can be repaired by direct joining mechanisms. The major repair pathway is the classical c-NHEJ, which is active throughout the cell cycle without requiring sequence homologies. This pathway employs the products of Ku70/80 heterodimers (XRCC6/5), DNA-dependent protein kinase catalytic subunit (DNA-PKcs), Artemis, DNA Ligase IV (LIG4) complex, consisting of DNA Lig4 and its cofactor X-ray repair cross-complementing protein 4 (XRCC4), and XLF (XRCC4-like factor, also called Cernunnos) [4]. Recently, the alternative alt-NHEJ pathway has been identified that does not utilize c-NHEJ factors and is mediated by PARP1, DNA Ligase IIIα (Lig3) or DNA Ligase I (Lig1)[5,6]. Both pathway have non-conservative nature, but while c-NHEJ generally restores chromosome integrity without rearrangements, alt-NHEJ has low fidelity end-joining with frequent microhomologies [7]. In particular, PARP-1 and DNA ligase 3 (Lig 3) are involved in a sub pathway of alt-NHEJ termed microhomology mediated end joining (MMEJ) that rejoins the ends by base pairing between microhomologous sequence, whereas DNA ligase 1(Lig1) mediates the ligation step in alt-NHEJ events that do not rely on such microhomologies [8,9]. Emerging evidence have demonstrated that alt-NHEJ can also occur in c-NHEJ-proficient cells [10], moreover, alt-NHEJ pathway can mediate end-joining in cells deficient in NHEJ, although alt-NHEJ is kinetically slower and less accurate than NHEJ [11].

The inherent DSB repair capacity of tumor cells can limit the effectiveness of radiotherapy, contributing to radioresistant phenotypes. Recent evidences from clinical trials in radiotherapy highlighted that increasing the dose can lead to reduced survival and a decline of quality of life [12,13], suggesting the need to develop agents that can be combined with radiotherapy in preclinical models. Different drug radiotherapy combinations have been investigated, and most are unfortunately associated with increased toxicity [14,15].

In the current study, we investigated on the combination of microRNA-mediated targeting of DSB repair genes along with IR as a strategy to sensitize non-small cell lung cancer (NSCLC) cells to the cytotoxic effects of IR. MicroRNAs (miRNAs) are 18–24 nt endogenous and natural occurring non-coding RNAs that negatively regulate gene expression by binding to the complementary sequence in the 3'-untranslated region (UTR) of target genes. MiRNAs have a pivotal role as post-transcriptional regulators of gene expression through the repression of target mRNAs that leads to decreased translational efficiency and/or decreased mRNA levels [16]. Several studies suggested that miRNA expression is regulated during the DNA-Damage response at the transcriptional level, in a p53-dependent manner [17], and through modulation of miRNAs processing and maturation steps [18]. The relationship between DDR genes and radioresistance has long been established, nevertheless, little is known about the miRNA-mediated regulation of HR and NHEJ pathway during the IR-response of human non-small cell lung cancer (NSCLC) cells. NSCLC is the most common type of lung cancer, accounting for approximately 80% of all lung cancer cases and with a very low (~18%) 5-year survival rate [19]. Radioresistance in NSCLC, either intrinsic or acquired, represents a critical barrier for the maximal efficacy of radiotherapy. Factors associated with radioresistance in NSCLC, include overexpression of PIM1 and reduction of protein phosphatases (PP2A and PP5), which induced translocation of PIM1 into the nucleus [20]. Recently, Wang and colleagues [21] identified several differences in protein expression, especially in DNA damage repair pathways, between radiosensitive and radioresistant NSCLC cell lines.

In the current study, we hypothesized that miRNA-mediated down-regulation of target genes having a central role in HR and NHEJ would sensitize NSCLC cells to IR. Before testing the capability of selected miRNAs as agents able to promote cellular sensitivity to IR, we functionally validated miRNA-mRNA interactions involving essential genes of HR (*RAD51*, *BRCA2*) and NHEJ (*PRKDC*, *XRCC5*, *LIG1*). We chose the *TP53* wild type NSCLC cells, A549 and NCI-H2347 [22, 23], to ascertain that DDR pathway and DNA repair were not influenced by *TP53* status, that is commonly mutated in lung cancer, ranging from 33% in adenocarcinomas to 70% in small cell lung cancers [24]. Moreover, TP53 tumor-suppressor family members participate in the regulation of miRNA expression at both the transcriptional and post-transcriptional levels [25]. The contribution

of HR and NHEJ repair when each pathway is chemically inhibited with specific inhibitors has been examined to evaluate the impact of selected miRNAs in DSB repair of NSCLC cells.

2. Materials and methods

2.1. Cell Culture and reagents

All culture medium were from Life Technologies (Carlsbad, CA, USA) and were supplemented with heat inactivated fetal bovine serum (FBS, BIOCHROM, Berlin, Germany), 38 units/mL streptomycin, and 100 units/mL penicillin G. All cells were grown at 37◦C in a humidified atmosphere with 5% CO_2. Non-small cell carcinoma cells were purchased from the American Type Culture Collection (ATCC, Manassas, VA). A549 cells derived from human alveolar type 2 primary lung adenocarcinoma cells (CCL-185™) and were cultured in Ham's F12-K Nutrient Mixture; NCI-H2347 cells derived from stage-1 adenocarcinoma (CRL-5942™), and were cultured in RPMI 1640 Medium supplemented with GlutaMAX™. Human glioma cells M059J were purchased from ATCC (CRL-2366™), whereas M059K cells were kindly provided by Professor S.C. West (Cancer Research UK London Research Institute, Clare Hall Laboratories, South Mimms, UK). Both cell lines were grown in a 1:1 mixture of DMEM and Ham's F-12 medium (DMEM/F-12, Gibco, Life Technologies), HEPES 20 mM, 1% of MEM non-essential amino acids and 10% of heat-inactivated FCS. Cells were kept at 37 °C in a humidified atmosphere of 95% air and 5% CO2, and maintained in exponential and asynchronous phase of growth by repeated trypsinization and reseeding prior to reaching subconfluency. The cells were tested to confirm that they were free of *Mycoplasma* by detecting the presence of mycoplasma in cell culture supernatants by PCR amplification using the N-GARDE Mycoplasma PCR Reagent set (Euroclone).

To specifically inhibit NHEJ or HR pathways, A549 cells were incubated with NU7026 (DNA-PKcs inhibitor, Sigma-Aldrich), RI-1 (RAD51 inhibitor, Sigma-Aldrich), or L67 (LIG III and LIG I inhibitor, Axon) diluted in DMSO at the final concentration of 5 μM for clonogenic assays and 10 μM for DSB repair assay. Incubation with inhibitors started 24 h before irradiation; after irradiation, the medium was replaced with a fresh one containing the inhibitor, and the cells were incubated thereafter.

2.2. Cell irradiation

Cells were seeded on Petri dishes (35x15 or 60x15 mm), with or without glass coverslips, kept on ice before and after irradiation, and cultured at 37° C in fresh medium thereafter. Irradiation with γ-rays was performed at the Department of Oncological and Surgical Sciences of Padova University with a 137Cs source (dose rate of 2.8 Gy/min) within the dose range 0-6 Gy. Except for irradiation, the control cells were subjected to the same experimental conditions.

2.3. Cell transfection

Twenty-four hours prior to transfection, cells were plated in 3.5-cm culture dishes at 40%–60% confluence. A549 cells were transfected with mirVana™ miRNA mimics (hsa-miR-96-5p, hsa-miR-874-3p), Pre-miR miRNA Precursor (hsa-miR-19a-5p, hsa-miR-144-3p, hsa-miR-182-5p, hsa-miR-218-5p, hsa-miR-342-3p) and Pre-miR™ Negative Control #1 (all from Ambion Austin, TX, USA) by using Lipofectamine™ 2000 (Invitrogen Life Technologies, Carlsbad, CA, USA) for luciferase assays, or Hiperfect Transfection Reagent (QIAGEN, Hilden, Germany) for miRNA over-expression, according to manufacturer's protocol. The sequence of miRNA mimics is reported in supplementary Table S1. Mock-transfected cells underwent the transfection process without addition of miRNA (i.e., cells were treated with transfection reagent only). The medium was replaced 4–6 h after transfection with new culture medium. Transfections were performed in triplicate for each experiment and repeated 3–4 times.

2.4. Total RNA isolation

Total RNA was isolated from irradiated and non-irradiated cells by using Trizol® Reagent (Invitrogen, Life Technologies, Carlsbad, CA, USA), according to the manufacturers protocol. Total RNA quantification was performed using the ND-1000 spectrophotometer (Nanodrop, Wilmington, DE, USA); RNA integrity and the content of miRNAs were assessed by capillary electrophoresis using the Agilent Bioanalyzer 2100, with the RNA 6000 Nano and the small RNA Nano chips, respectively (Agilent Technologies, Palo Alto, CA, USA). Only total RNA samples with RNA Integrity Number (RIN) values ≥ 6 were used for microarray analysis.

2.5. MiRNA profiling and data processing

MiRNA expression profiles were carried out in irradiated vs. non-irradiated A549 cells at 4 and 24 h after irradiation with 2 Gy by using the "SurePrint G3 Human miRNA r21 Array kit" (Agilent

Technologies), that allows the detection of 2.549 human (miRBase database Release 21.0) and 76 human viral miRNAs. Four different samples of cells (irradiated and non-irradiated) have been analyzed for each time point according to protocols previously described [26]. Briefly, total RNA (200 ng) was labeled with pCp Cy3, according to the Agilent protocol and unincorporated dyes were removed with MicroBioSpin6 columns (BioRad) [27]. Probes were hybridized at 55°C for 22 hours using the Agilent's Hybridization Oven that is suited for bubble-mixing and microarray hybridization processes. Then, the slides were washed by Agilent Gene expression wash buffer 1 and 2 and scanned using an Agilent microarray scanner (model G2565CA) at 100% and 5% sensitivity settings. Agilent Feature Extraction software version 10.5.1.1 was used for image analysis. Inter-array normalization of expression levels was performed with cyclic Lowess for miRNA experiments and with quantile for gene expression profiling [28] to correct possible experimental distortions. Normalization function was applied to expression data of all experiments and then values of spot replicates within arrays were averaged. Furthermore, Feature Extraction Software provides spot quality measures in order to evaluate the goodness and the reliability of hybridization. In particular flag ''gIsFound'' (set to 1 if the spot has an intensity value significantly different from the local background, 0 otherwise) was used to filter out unreliable probes: flag equal to 0 will be noted as ''not available (NA)''. So, in order to make more robust and unbiased statistical analysis, probes with a high proportion of ''NA'' values were removed from the dataset. We decided to use the 40% of NA as threshold in the filtering process obtaining a total of 270 available human miRNAs. Principal component analysis, cluster analysis and profile similarity searching were performed with tMev that is part of the TM4 Microarray Software Suite [29]. The expression level of each miRNA and mRNA was calculated as the log 2 (irradiated/non-irradiated cells). The raw data of microarray have been deposited on the Gene Expression Omnibus (GEO) website (http://www.ncbi.nlm.nih.gov/geo/) using accession number GSE112376.

2.6. Quantitative real time-PCR (qRT-PCR)

For mRNA detection 1 μg of total RNA was retrotranscribed with ImProm-II Reverse Transcription System (Promega, Madison, WI, USA) as previously described [26]. qRT-PCR reactions were performed with the Go Taq qPCR Master Mix (Promega, Madison, WI, USA) and performed in triplicates. Gene-specific primers for *RAD51*, *BRCA1*, *BRCA2*, *PRKDC (DNA-PKcs)*, *XRCC4*, *XRCC5 (KU80)*, *XRCC6 (KU70)*, *LIG1*, *LIG4*, *DDB2*, *GADD45A*, *CDKN1A*, *ATM*, *TP53* and *GAPDH* are available at supplementary Table S2. The data of miRNA expression analysis were validated by using the TaqMan® MicroRNA Assay kit (Applied Biosystems, Foster City, CA), as

previously reported [26]. In brief, each RT reaction contained 10 ng of total purified RNA, stem-loop RT primer, RT buffer, 0.25 mM each of dNTPs, 50 U MultiScribe™ reverse transcriptase and 3.8 U Rnase inhibitor. The reactions were incubated in a Mastercycler EP gradient S (Eppendorf) in 0.2 μl PCR tubes for 30 min at 16°C, 30 min at 42°C, followed by 5 min at 85°C, and then held at 4°C. The resulting cDNA was quantitatively amplified in 40 cycles on an ABI 7500 Real-Time PCR System, using TaqMan Universal PCR Master Mix and Taqman MicroRNA Assays for hsa-miR-210-3p, hsa-miR-19a-3p, hsa-miR-182-5p and for U48 small nuclear (RNU48) as endogenous control. The relative expression levels of genes and miRNAs were calculated using the comparative delta Ct (threshold cycle number) method (2^{-ddCt}) [30] implemented in the 7500 Real Time PCR System software (Applied Biosystems® 7500 Real-Time PCR System, Life Technologies, Carlsbad, CA, USA, 2007).

2.7. Construction of Recombinant Vectors and site-directed mutagenesis

The partial 3'UTR of genes *RAD51*, *PRKDC*, *LIG1*, was amplified by PCR from human cDNA and cloned into the pmirGLO Dual-Luciferase miRNA Target Expression Vector (Promega, Madison, WI), immediately downstream of the firely luciferase gene as previously described [26]. The sequence of each insert was confirmed by sequencing. To predict base-pairing for miRNA-mRNA interaction, we used Targetscan algorithm [31,32], that predicts biological targets of miRNAs by searching for the presence of conserved sites that match the seed region of each miRNA. The 3'UTR was mutagenized at the miRNA recognition sites using the Quick Change Site-Directed Mutagenesis kit (Stratagene, Agilent Technologies, Santa Clara, CA, USA) according to manufacturer's instructions. Primers used for the cloning of *RAD51*, *BRCA2*, *PRKDC*, *XRCC5*, *LIG1*, wild type and mutated are available at supplementary Table S3.

2.8. Dual-Luciferase Reporter Assay

A549 cells were plated in 24-well plates (14×10^5 cells/well) and 24 h later co-transfected with 50 ng of the pmirGLO dual-luciferase constructs, containing the 3'UTR of genes, and with 32 nM pre-miR™ miRNA Precursor (miRNA mimics) or pre-miR™ miRNA Precursor Molecules-Negative Control (Control mimic) (Ambion, Austin, TX, USA), using Lipofectamine™ 2000 (Invitrogen Life Technologies, Carlsbad, CA, USA). Lysates were collected 24-48 h after transfection and Firefly and Renilla Luciferase activities were consecutively measured by using Dual-Luciferase Reporter Assay (Promega, Madison, WI, USA), according to manufacturer's instructions. Firefly

luciferase signal was normalized against the internal control Renilla luciferase. Relative luciferase activity was calculated by normalizing the ratio of Firefly/Renilla luciferase to that of negative control-transfected cells (mock). Transfections were performed in triplicate and repeated 3–4 times.

2.9. Clonogenic Survival Assay

A549 were seeded in 3.5-cm culture dishes and allowed to attach overnight, then were subjected to transfection with miRNA mimics 32nM and 24 h later irradiated with γ-rays. After irradiation, cells were harvested by trypsinization and counted by trypan blue dye exclusion. For the colony-forming assay 300 viable cells were plated in 6-cm culture dishes in a mixture of conditioned medium and fresh complete medium (1:1) and grown for 10-12 days. After verification of visible colony formation cells were stained with 0.25% crystal violet in 100% methanol, and colonies of ≥ 50 cells were quantified. Cell survival was calculated as percentage of cloning efficiency (C.E.) of irradiated miRNA-transfected cells over that of their respective non-irradiated mock control cells (i.e. cells transfected with only lipofectamine). Cell survival was measured in cells transfected with pre-miR™ Negative Control to ensure that biological effects was correctly interpreted.

2.10. Cell cycle analysis

The cell cycle distribution of irradiated and non-irradiated control cells was assessed by flow cytometry analysis of DNA content following staining with propidium iodide (PI, Sigma-Aldrich), as previously described [33]. The samples were analyzed using a BD FACSCanto™ II flow cytometer (BD Biosciences); data from 10×10^3 cells/sample were collected for acquisition and cell cycle distribution analysis using Cell Quest (version 3.0, BD Biosciences) and ModFit LT 3.0 software (BD Biosciences), respectively.

2.11. Cellular extracts and sub-cellular fractionation

Cellular extracts were prepared from irradiated and non-irradiated cells at 4 and 24 h after irradiation. Whole-cell extracts from 1 x 10^6 cells were prepared in radio-immunoprecipitation assay (RIPA) lysis buffer (50 mM Tris, pH 7.4, 150 mM NaCl, 1% NP-40, 1 mM NaF, 1 mM EDTA, 1 mM Na3VO4, 1 mM PMSF, 0.25% Na-deoxycholate, and 5 U/ml aprotinin). Cytosolic and nuclear extraction of proteins was performed by using the CelLytic™ NuCLEAR™ Extraction kit (Sigma-Aldrich), according to manufacturer's indications. Briefly, cells were suspended in Lysis

Buffer 1X, containing DTT and protease inhibitors, incubated on ice 15 min allowing cells to swell and, to the swollen cells was add 10% IGEPAL CA-630 solution to a final concentration of 0.6%. Cells were vortexed and centrifuged at 10.000g and cytosolic fraction was recovered. The nuclei pellet was resuspended in Extraction Buffer, containing DTT and protease inhibitors, centrifuged at 21.000 g for 5 min and supernatant containing the nuclear fraction was collected.

2.12. Western blotting

Cell lysates were quantified by Bradford assay at the spectrophotometer (Eppendorf BioSpectrometer® basic) and then 20 μg of lysates were separated on Mini-PROTEAN® TGX™ Precast Gels (BIO-RAD) and transferred to nitrocellulose membranes (Hybond-C Extra; Amersham, GE Healthcare). Membranes were probed with primary antibodies anti-RAD51 (Santa Cruz Biotechnology, H-92: sc-8349, lot. G0811, 1:100), anti-KU80 (Cell Signaling, #2753, 1:1000), anti-DNA Ligase I (Genetex International, 1:200), anti-DNA-PKcs (Abcam, clone Y393, 1:200), anti-α tubulin (Santa Cruz Biotechnology, B-7: sc-5286, 1:10.000), anti-HDAC (Santa Cruz: sc-7872, 1.1000) and then incubated with Amersham ECL horseradish peroxidase-conjugated secondary antibodies (GE Healthcare, 1:40.000). Resulting immunoreactive bands were detected using enhanced chemioluminescent HRP substrate (Millipore) and analyzed by ImageQuant LAS 4000 mini (GE Heathcare). The bands' intensities were quantified with ImageJ software and normalized utilizing α-tubulin as endogenous reference protein.

2.13. DSB repair assay

To evaluate the induction and repair of DSBs we monitored the kinetics of γ-H2AX. At different times after irradiation (0.5, 2, 6, and 24 h) the non-irradiated and irradiated cells were fixed with a 4% solution of formaldehyde (Sigma-Aldrich) as previously described [34]. After permeabilization in 0.2% Triton X-100–PBS and blocking in 10% goat serum–PBS, the cells were incubated for 2 h at room temperature with anti-γ-H2AX (Ser139) (Millipore Chemicon Upstate Clone JBW301, 1:100). The cells were then incubated at room temperature for 1 h with secondary antibodies Alexa Fluor® 488 goat anti-mouse and Alexa Fluor® 594 donkey anti-rabbit (Life Technologies, 1:350) and washed, as described elsewhere. Nuclei were stained with 2 μg/ml DAPI (4′,6-diamidino-2-phenylindole) in antifade solution (Vectashield, Vector Laboratories), and cover glass slips were mounted. Images of foci were captured using a Leica TCS SP5 confocal microscope (Leica Microsystems) with a 63X oil immersion objective. All the images were acquired under the same

conditions of laser intensity, PMC voltage, pinhole aperture, and optical slice (0.5 μm) and processed by Adobe Photoshop 8.0 software (Adobe). For each experimental point, foci were scored by eye from at least 250 nuclei.

2.14. Statistical and bioinformatics analyses

The results are reported as the mean ± standard error (S.E.) or standard deviation (S.D.). The differences between groups were evaluated by two-tailed, unpaired Student's *t*-test and differences with a *p*-value < 0.05 were considered significant. The identification of differentially expressed genes and miRNAs was performed with Multi Experiment Viewer – version 4.9.1 one and two class Significance Analysis of Microarray (SAM) program [35] with default settings. To predict the target genes of differentially expressed miRNA targets we have performed a computational analysis by using Targetscan v 6.2 (http://www.targetscan.org/) [31, 32]. For Gene Ontology (GO) and KEGG analyses on differentially miRNAs we used DIANA-miRPath v3.0 [36] that extends the Fisher's Exact Test, EASE score and False Discovery Rate methodologies, with the use of unbiased empirical distributions.

2.15. Ethical approval

All the studies were performed using commercially available cell lines and did not require any specific approval.

3. Results

3.1. Innate radiosensitivity of NSCLC cells

We assessed the innate sensitivity to radiation of NSCLC A549 and NCI-H2347 cells by analyzing their proliferation ability after irradiation with increasing doses of γ-rays. Cloning forming ability was assessed in exponentially growing cells after irradiation with 1, 2, 3 Gy and, for comparison, in human glioma cells with a well-known radiation sensitivity: M059K (DNA-PKcs proficient, radioresistant) and M059J (DNA-PKcs deficient, radiosensitive) cell lines established from the same tumor [37]. A549 and NCI-H2347 cells displayed high values of cell survival after irradiation, being able to form colonies after all IR doses, even at 3 Gy, similarly to radioresistant M059K cells

(Figure 1 A). The effect of irradiation on cell proliferation ability was further examined by flow-cytometry cell cycle analyses of exponentially growing cells irradiated with increasing doses of γ-rays (2, 4, 6 Gy) and harvested at 6 and 24 h after irradiation (Figure 1 B-D). Six hours after irradiation A549 cells showed a G2-phase arrest (27% of G2-cells in 2 Gy cells *vs.* 11% of G2-cells in 0 Gy cells) whereas NCI-H2347 cells and M059K cells accumulated mainly in S-phase. The fraction of S-phase cells was approximately 10% greater in irradiated than in non-irradiated NCI-H2347 and M059K cells. Twenty-four hours after irradiation NCI-H2347 cells showed a dose-dependent G2-phase arrest that was pronounced at the highest doses (36% at 4 Gy and 47% at 6 Gy *vs.* 11% in 0 Gy cells). On the contrary, at 24 h after irradiation A549 cells did not show a dose-dependent G_2-phase arrest and the proportion of G_1-phase cells increased to control levels, similarly to radioresistant M059K cells. No increase in the sub-G_1 fraction was observed in irradiated A549 cells (Figure 1 E), in accordance with the small fraction of apoptotic cells assessed by DAPI staining at 24 h after irradiation with 2 Gy (data not shown). A549 cells have confirmed a high tolerance to radiation as recently reported [21], and have been studied in further functional validation studies.

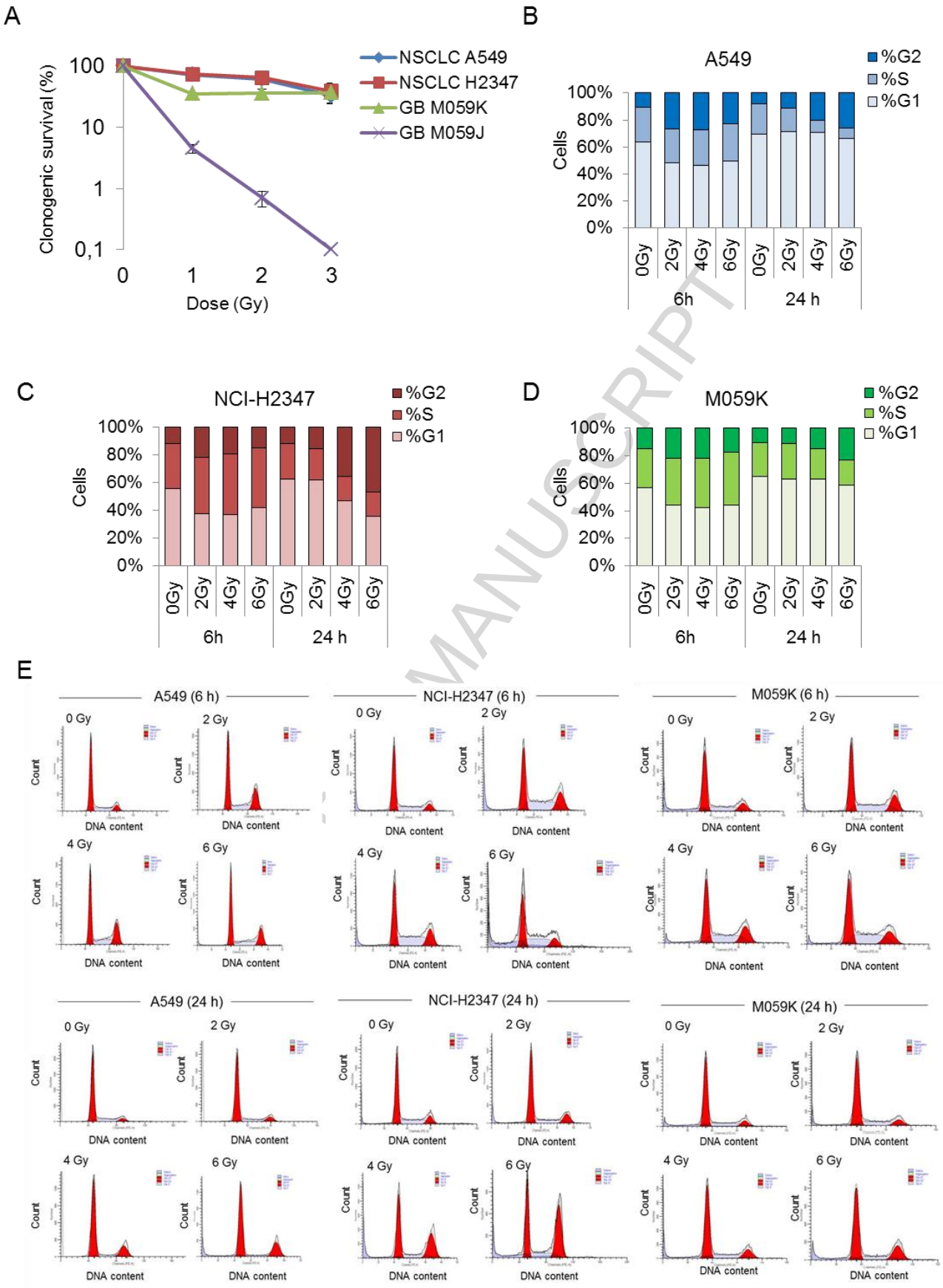

Figure 1. Innate radiosensitivity of NSCLC cells. A) Cell survival assessed by colony forming ability after irradiation with γ-rays (1, 2, 3 Gy) in A549 and NCI-H2347 and, for comparison, in glioblastoma (GB) M059K (DNA-PKcs proficient) and M059J (DNA-PKcs deficient) cells. Cell survival rate was calculated as the percentage of cloning efficiency of irradiated cells with respect to that of non-irradiated control cells (0 Gy). Data refer to means ± S.D. of independent experiments ($6 \leq n \leq 10$) carried out in quadruplicate. B-D) Cell cycle analysis by flow cytometry in non-irradiated and irradiated cells recovered at 6 and 24 h after irradiation with 2, 4, 6 Gy. Data were collected from 20.000 cells/sample using a BD FACSCanto™ II flow cytometer. E) Representative plots of cell cycle analysis in non-irradiated and irradiated cells are shown.

3.2. Gene and miRNA expression analyses in γ-irradiated NSCLC cells

Since our goal was to identify miRNA-mRNA interactions of DSB repair we analyzed the expression level of genes representative for HR pathway (*RAD51*, *BRCA1*, *BRCA2)*, and NHEJ pathway (*PRKDC*, *XRCC6*, *XRCC5*, *XRCC4*, *LIG1*, *LIG4)* at 4 and 24 h after irradiation with 2 Gy, *i.e.* the dose delivered daily in conventional fractionated radiation therapy protocols. As shown in Figure 2 the gene expression level was slightly affected in irradiated compared with non-irradiated cells at both times after IR, except for *XRCC6* (*KU70*) that was 2-fold induced at 4 h after IR.

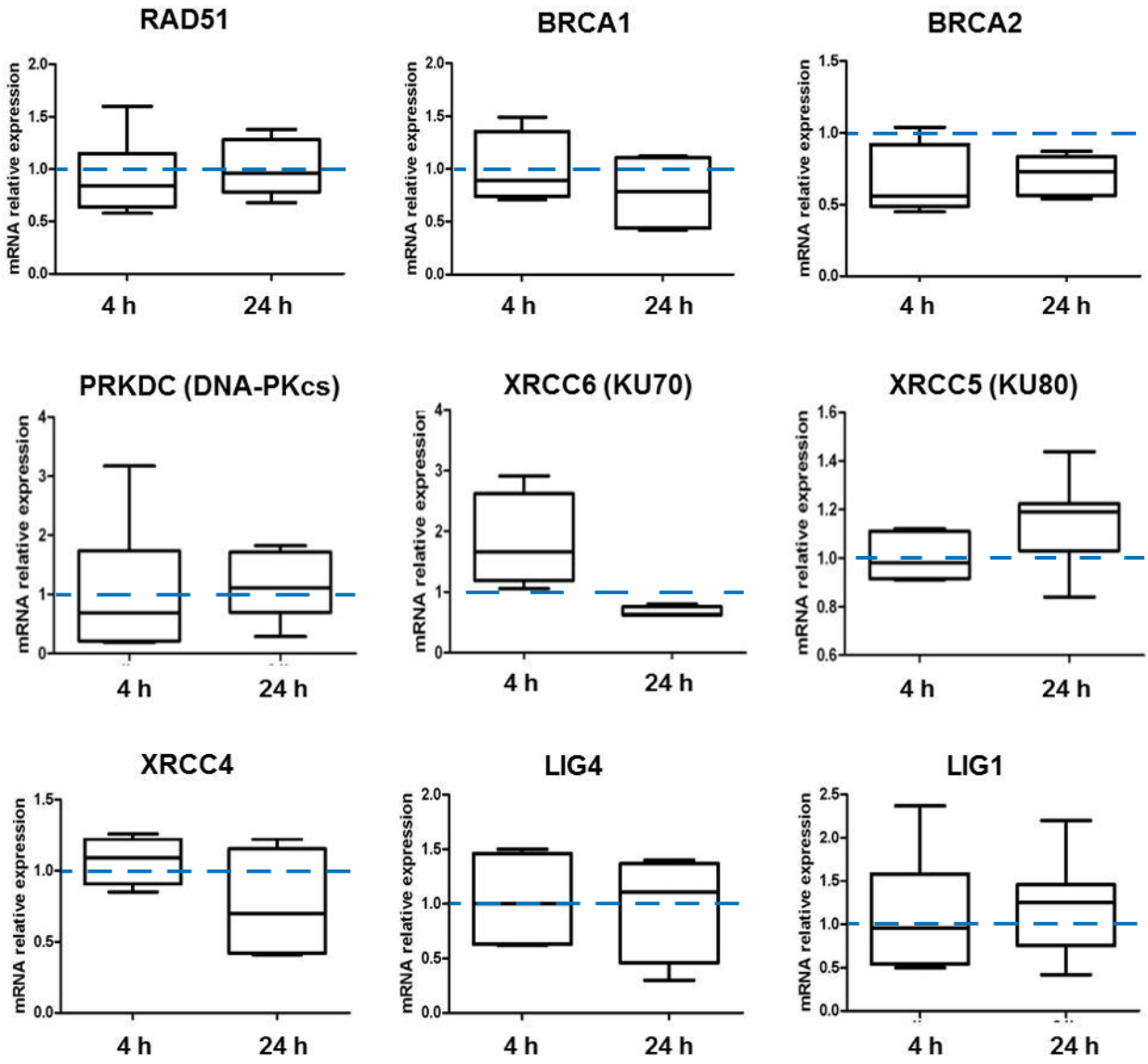

Figure 2. Expression analysis of DSB genes in γ-irradiated NSCLC A549 cells. The relative expression of each transcript has been determined by qRT-PCR at 4 and 24 h after irradiation with 2 Gy of γ-rays. Values (mean ± S.D.) of at least three independent experiments, each performed in triplicate, are expressed as fold-change of irradiated (2 Gy) *vs.* non-irradiated (0 Gy) control cells. The dotted blue line represents the value "1" of control cells when no change is observed.

We then evaluated the extent of miRNA response of NSCLC cells upon irradiation by performing miRNA expression profiling on total RNA extracted at 4 and 24 h after irradiation by comparing the expression profile of irradiated (2 Gy) *vs* non-irradiated (0 Gy) cells. Analyses allowed to identify 7 and 45 miRNAs differentially expressed, respectively at 4 and 24 h after irradiation (Figure 2). On the whole, the extent of expression change of differentially expressed miRNAs was small, being approximately lower than ~1.8-fold in irradiated compared with non-irradiated control cells. Raw

data and means of miRNA expression values are available at supplementary Tables S4-S5, together with microarray data validation by quantitative real-time polymerase chain reaction (qRT-PCR) of hsa-miR-210-3p, hsa-miR-19a-3p and hsa-miR-182-5p (supplementary Figure S1).

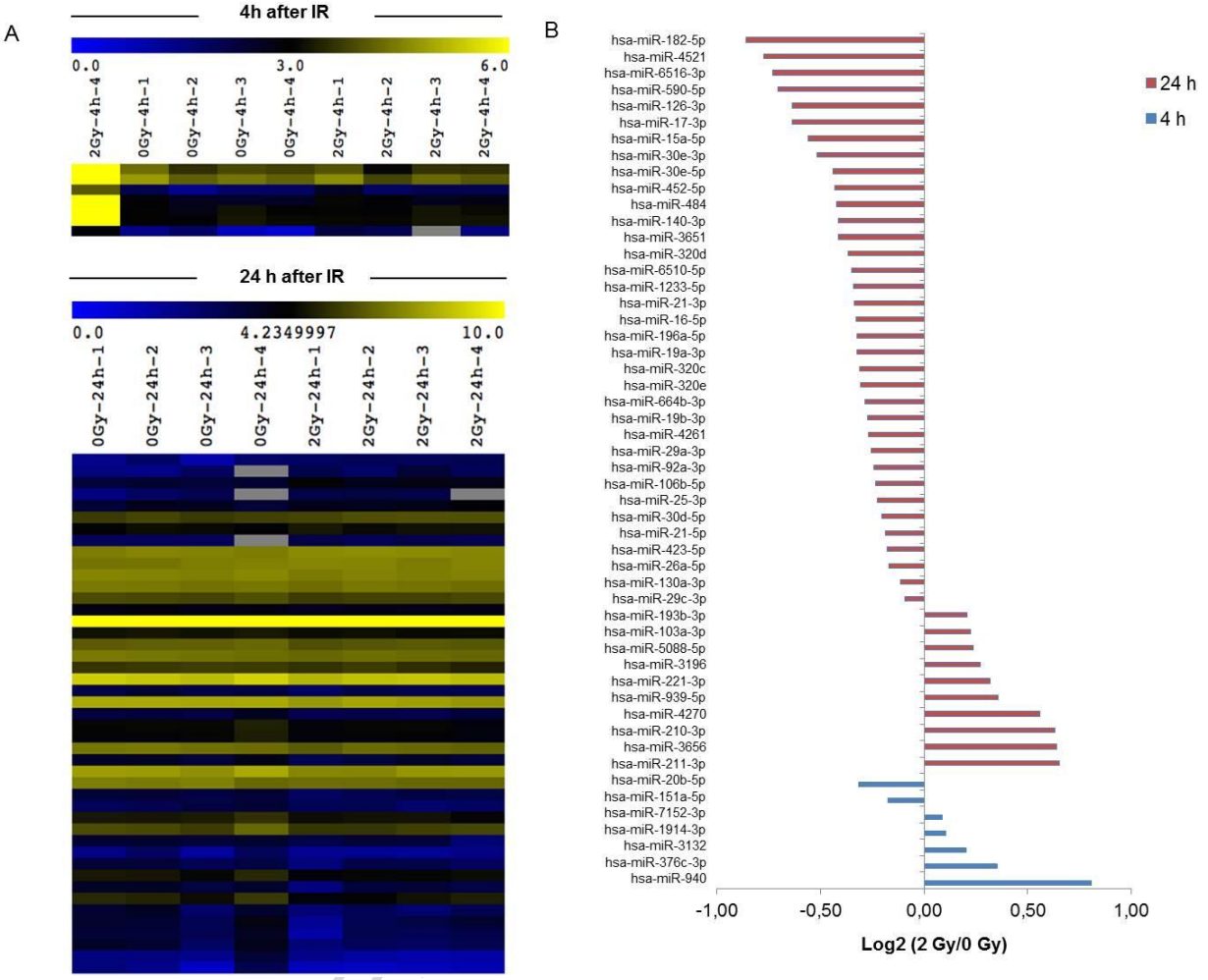

Figure 3. Differentially expressed miRNAs in γ-irradiated versus non-irradiated NSCLC A549 cells. Heatmap with radio-responsive miRNAs at 4 and 24 h after irradiation with 2 Gy (A). The range of expression value is from 0 (blu, down-regulation) to 10.0 (yellow, up-regulation). Grey boxes correspond to not available fluorescent signal from the microarray platform. Four biological replicates for each condition (irradiated and non-irradiated) have been analyzed. B) The expression value of each miRNA is the mean ± S.D. of expression values from four independent experiments calculated as the log2 ratio (2 Gy/0 Gy).

Subsequently, we investigated the biological significance in cellular pathways and molecular functions of differentially expressed miRNAs through enrichment analysis on Gene Ontology (GO). GO categories significantly enriched in cells harvested at 4 and 24 h after irradiation are reported in

Figure 3. Functional enrichment analysis identified components of different GO term belonging to general biological process, as for example response to stress (GO:0006950), membrane and extracellular matrix organization (GO:0061024; GO:0030198), cytoskeleton organization (GO:0007010), immune system process (GO:0002376). Biological categories of gene expression (GO:0010467), DNA-Damage response (GO:0006977), cell cycle (GO:0007049) and cell death (GO:0008219), were significantly enriched at both times after irradiation but with higher extent at 24 than at 4 h after irradiation. KEGG pathway analysis reported that the p53 signaling pathway was enriched at both 4 and 24 h after IR (supplementary Tables S6-S7), with respectively 20 and 60 genes (Figure 4 A). We validated the p53-related genes derived from the KEGG pathway analysis by measuring the expression level of representative genes of such pathway: *TP53* and *ATM*, according to their central role in this pathway, *DDB2*, *GADD45A*, and *CDKN1A* (p21) known to be radioresponsive genes [26, 38–42]. Figure 4 B shows that *GADD45A* and *CDKN1A* were ~3-fold induced at 4 h after IR, whereas *DDB2* and *ATM* were ~1.7-fold induced. At 24 h after IR the expression level of all genes decreased to control levels except for *CDKN1A* that was 1.8-fold up-regulated. The expression level of *TP53* was, on the whole, unaffected by radiation.

GO Term		Annotation	# genes at 4h	# genes at 24h
GO:0009058		biosynthetic process	513	1137
GO:0006464		cellular protein modification process	371	706
GO:0000278		mitotic cell cycle	64	189
GO:0009056		catabolic process	261	588
GO:0019899		enzyme binding	238	434
GO:0022607		cellular component assembly	165	419
GO:0006950		response to stress	284	631
GO:0061024		membrane organization	90	219
GO:0030198		extracellular matrix organization	0	115
GO:0006605		protein targeting	36	87
GO:0005768		endosome	76	166
GO:0007010		cytoskeleton organization	79	158
GO:0006629		lipid metabolic process	20	260
GO:0070062		extracellular vesicular exosome	0	821
GO:0000209		protein polyubiquitination	70	44
GO:0002376		immune system process	0	404
GO:0045087		innate immune response	80	182
GO:0006461		protein complex assembly	474	252
GO:0051403		stress-activated MAPK cascade	0	24
GO:0007165		signal transduction	499	0
GO:0016301		kinase activity	138	0
GO:0006810		transport	0	829
GO:0010467		**gene expression**	114	269
GO:0006325		chromatin organization	0	66
GO:0044822		poly(A) RNA binding	233	484
GO:0006367		transcription initiation from RNA polymerase II promoter	0	71
GO:0006397		mRNA processing	67	141
GO:0016071		mRNA metabolic process	0	92
GO:0031124		mRNA 3'-end processing	0	15
GO:0006283		transcription-coupled nucleotide-excision repair	0	18
GO:0006415		translational termination	0	33
GO:0000083		regulation of transcription involved in G1/S transition of mitotic cell cycle	8	11
GO:0006977		**DNA damage response**	12	27
GO:0006297		nucleotide-excision repair	0	11
GO:0006986		response to unfolded protein	15	26
GO:0006259		DNA metabolic process	0	254
GO:0016874		ligase activity	0	145
GO:0008219		**cell death**	130	301
GO:0006915		apoptotic process	102	220
GO:0043066		negative regulation of apoptotic process	91	175
GO:0043065		positive regulation of apoptotic process	0	117
GO:1900740		positive regulation of protein insertion into mitochondrial membrane involved i	8	20
GO:0097193		intrinsic apoptotic signaling pathway	15	35
GO:0097190		apoptotic signaling pathway	20	44
GO:0001836		release of cytochrome c from mitochondria	0	16
GO:0006921		cellular component disassembly involved in execution phase of apoptosis	0	22
GO:0007049		**cell cycle**	0	259
GO:0007067		mitotic nuclear division	64	107
GO:0000082		G1/S transition of mitotic cell cycle	29	69
GO:0000086		G2/M transition of mitotic cell cycle	24	62
GO:0007077		mitotic nuclear envelope disassembly	9	21
GO:0031145		anaphase-promoting complex-dependent proteasomal ubiquitin-dependent pro	0	31
GO:0051439		regulation of ubiquitin-protein ligase activity involved in mitotic cell cycle	0	29
GO:0006271		DNA strand elongation involved in DNA replication	0	20

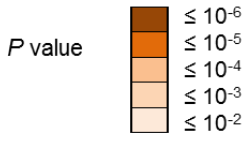

Figure 4. Gene Ontology (GO) analysis in γ-irradiated NSCLC cells. Biological processes found enriched from GO analysis are shown together with the number of putative target genes for each functional category. The color represents the relative *P* value significance which is determined by Fisher's exact test. GO categories with *P* value < 0.01 were considered significant.

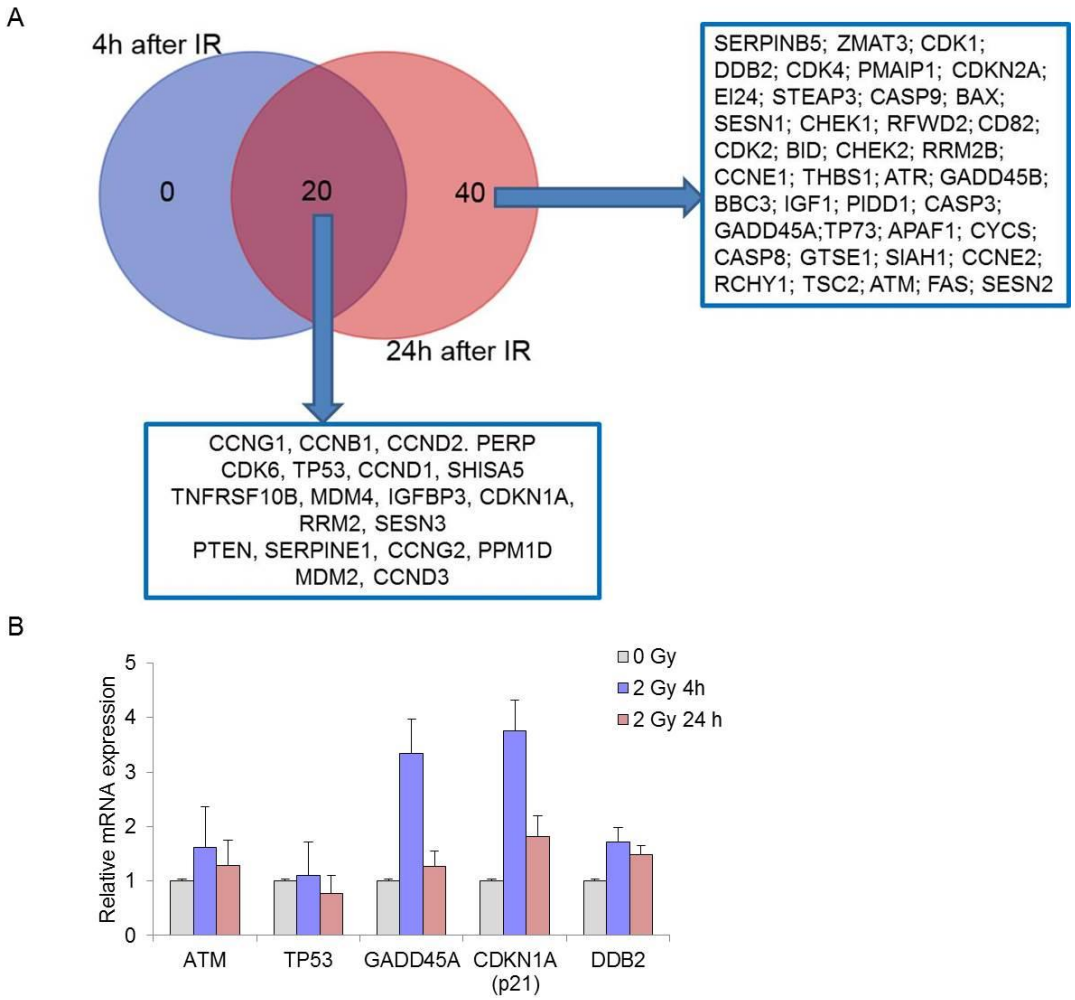

Figure 5. P53 signaling pathway enrichment in γ-irradiated NSCLC A549 cells. A) The Venn diagram shows the p53-related genes derived from KEGG pathway analysis at 4 and 24 h after irradiation (IR): twenty genes are common to both times after IR, whereas forty genes are enriched at 24 h after IR. B) Validation by qRT-PCR analyses of *TP53*, *ATM*, *DDB2*, *GADD45A*, and *CDKN1A* (p21) genes in 2Gy-irradiated A549 cells. Data are means ± S.D. of independent experiments carried out in cells recovered at 4 and 24 h after irradiation.

3.3. Functional validation of miRNA-mRNA interactions

We performed computational analyses by using the target prediction algorithm TargetScan 6.2 to predict target genes of differentially expressed miRNAs. Our interest was to find out and validate miRNA-mRNA interactions involved in DSB repair and to this purpose, we identified two differentially expressed miRNAs targeting DSB repair genes: hsa-miR-19a-3p and hsa-miR-182-5p, having as putative target genes *BRCA2* and *RAD51*, respectively. We thus constructed luciferase

vectors containing the 3'UTR of *BRCA2* and *RAD51* genes to determine whether they were direct targets of the two identified miRNAs by *in silico* analysis. We next sought to identify other miRNA-mRNA interactions of DSB repair taking into account i) the gene crucial role in repair pathway; ii) the conserved regions of miRNA during prediction analyses; iii) the differentially expressed miRNAs in NSCLC cells reported in literature. As possible IR-sensitizing target genes we chose *RAD51* and *BRCA2* of HR pathway, and *PRKDC*, *XRCC5*, *LIG1* of NHEJ. We investigated the interaction of *RAD51* with two candidate targeting miRNAs dysregulated in NSCLC: hsa-miR-96-5p [43,44] and hsa-miR-144-3p [44]. We tested the interaction between *XRCC5* and hsa-miR-218-5p that is a potential biomarker for lung adenocarcinoma [44] and the interaction between *PRKDC* and hsa-miR-874-3p, whose expression level is down-regulated in NSCLC [45]. According to prediction analyses also *LIG1* is a putative target gene of hsa-miR-874-3p, thus we tested this interaction together with that between *LIG1* and hsa-miR-342-3p, which is differentially expressed in NSCLC [46, 47]. MiRNA-mRNA interactions of DSB repair tested in functional studies are reported in Table 1**.**

Table 1. MiRNA-mRNA interactions of DSB repair analyzed for functional validation.

Gene	DSB pathway	Predicted miRNA
RAD51	Homologous Recombination (HR)	hsa-miR-182-5p hsa-miR-96-5p hsa-miR-144-3p
BRCA2	Homologous Recombination (HR)	hsa-miR-19a-3p
PRKDC (DNA-dependent protein kinase catalytic subunit, DNA-PKcs)	Non-homologous end joining, classical (c-NHEJ)	hsa-miR-874-3p
XRCC5 (X-ray repair cross-complementing protein 5, KU80)	Non-homologous end joining, classical (c-NHEJ)	hsa-miR-218-5p
LIG1 (DNA ligase I)	Non-homologous end joining, alternative (alt-NHEJ)	hsa-miR-874-3p hsa-miR-342-3p

We constructed luciferase vectors containing the 3'UTR of these genes for functional testing with the luciferase reporter assay. A549 cells were co-transfected with synthetic mimics of interest, or miRNA negative control, and expression vectors containing the 3'UTR of the target gene, cloned downstream of the luciferase gene. Figure 6 shows that hsa-miR-96-5p mimic reduced significantly the luciferase activity from constructs containing the RAD51 3'UTR, in contrast to hsa-miR-144-3p and hsa-miR-182-5p. Hsa-miR-874-3p, but not hsa-miR-342-3p, reduced significantly the luciferase

activity from constructs containing the LIG1 3'UTR, and also the PRKDC 3'UTR. Hsa-miR-19a-3p and hsa-miR-218-5p decreased significantly the luciferase activity from constructs containing the BRCA2 and XRCC5 3'UTR respectively.

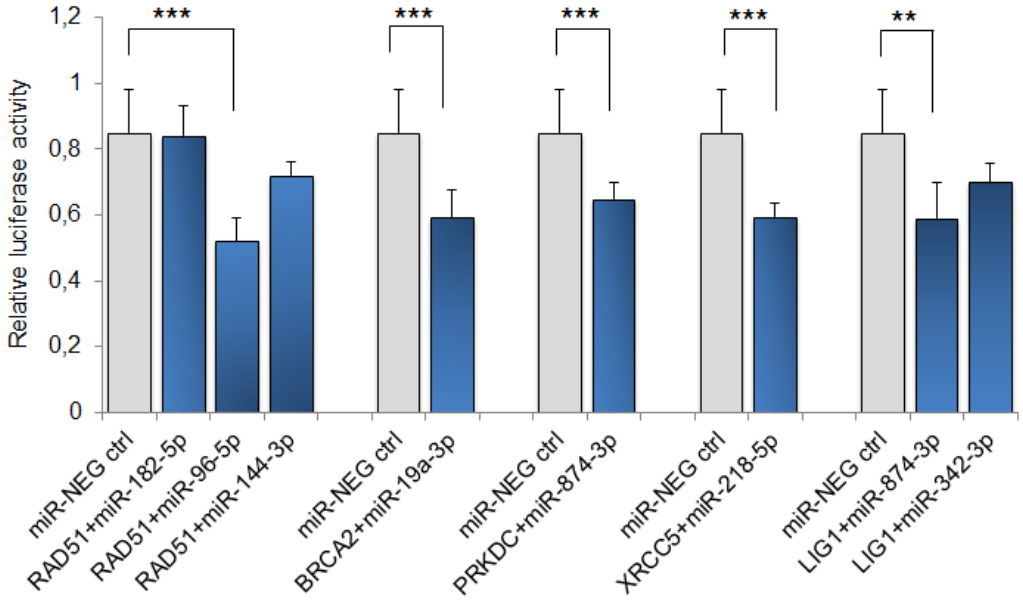

Figure 6. Luciferase assay for functional miRNA-mRNA interactions. The 3'UTRs of target genes *RAD51*, *BRCA2*, *PRKDC* (DNA-PKcs), *XRCC5* (KU80) and *LIG1* were cloned into Dual-Luciferase Reporter vectors for validation *in vivo*. A549 cells were co-transfected with the firefly luciferase reporter plasmid and with miRNA mimics or pre-miRNA precursor-Negative Control. Luciferase activity was assayed 48 h after transfection. The data represent mean ± S.D. from independent experiments ($3 \leq n \geq 5$), normalized on Renilla Luciferase activity (***$p < 0.001$; **$p < 0.01$; *t*-test).

Before performing further validation studies by site-directed mutagenesis on the identified significant miRNA-mRNA interactions, we tested the impact of hsa-miR-96-5p, hsa-miR-874-3p, hsa-miR-19a-3p, and hsa-miR-218-5p on cloning forming ability of irradiated A549 cells. Hsa-miR-96-5p and hsa-miR-874-3p decreased cell survival of irradiated cells, whereas hsa-miR-19a-3p and hsa-miR-218-5p little affected cell survival after irradiation (supplementary Figure 2). Based on these results, we performed experiments of site-directed mutagenesis to validate that hsa-miR-96-5p actually targets 3'-UTR of *RAD51* gene, and hsa-miR-874-3p targets 3'-UTR of *PRKDC* and *LIG1* genes. The luciferase constructs, containing wild type and mutated 3'UTR of such genes, were tested for miRNA interaction. As shown in Figure 7 the activity of the reporter construct containing

wild type RAD51-3'UTR was significantly decreased by the treatment with hsa-miR-96-5p mimic, whereas the construct with the mutated seed region of hsa-miR-96-5p was refractory to miRNA-mediated repression. Similarly, the luciferase activity of the reporter construct containing mutated LIG1-3'UTR and PRKDC-3'UTRs was refractory to hsa-miR-874-3p action.

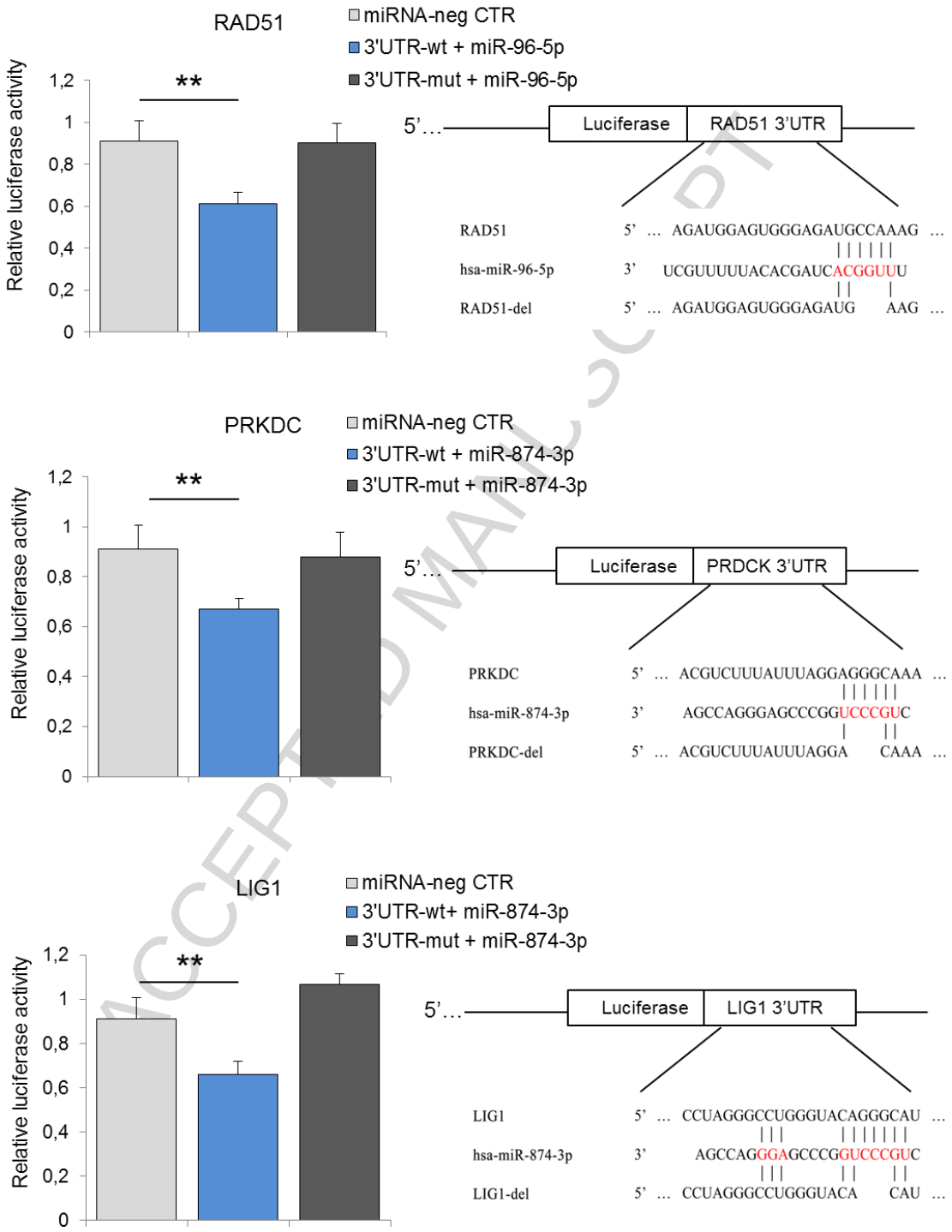

Figure 7. Site-directed mutagenesis. A549 cells were co-transfected with miRNA mimics or miRNA-negative control and with the Firefly luciferase reporter plasmid containing wild-type or

mutant 3'-UTR. Luciferase activity was assayed 48 h after transfection (**p<0.01, t-test). The putative regions of 3'-UTR for miRNA binding and corresponding mutant miRNA binding sites are shown in diagrams.

The ultimate validation of predicted miRNA targets is the biologic validation *in vivo*. To this purpose, we measured the expression level of RAD51, DNA-PKcs and LIG1 transcripts in miRNA-over-expressing A549 cells. As shown in Figure 8 A the expression level of target genes decreased significantly in cells over-expressing miRNAs irradiated with 2 Gy and recovered immediately after IR. We then investigated the effect of miRNAs on the expression levels of proteins RAD51, DNA-PKcs, and DNA-Ligase 1, in cells irradiated with 2 Gy and recovered at 4 and 24 h after IR. RAD51, DNA-PKcs, and DNA-Ligase 1 proteins were endogenously expressed in A549 cells, without differences between 2Gy-irradiated and non-irradiated cells. Hsa-miR-96-5p mimic decreased the expression level of RAD51 protein at 4 and 24 h after irradiation in whole lysates (Figure 8 B). The decreased expression level of RAD51 in non-irradiated cells (0 Gy) at 24 h after irradiation was related to the small proliferating fraction of cells deriving from confluent cells, accordingly to the threshold expression level of RAD51 that reflects the proliferating status of cells [48]. Over-expression of hsa-miR-874-3p mimic affected the level of DNA-PKcs at 24 h after IR in whole cell lysates whereas no effect on DNA-Ligase 1 expression was detected (Figure 8 C-D). The targeting effect of hsa-miR-96-5p on RAD51 protein expression was evident also in fractionated lysates (both cytosolic and nuclear) at 4 h and 24 h after irradiation (Figure 8 E). . The targeting effect of hsa-miR-874-3p mimic on DNA-PKcs was evident in nuclear extracts at both times after IR, whereas DNA-Ligase 1 protein expression mildly decreased in nuclear extracts at 24 h after IR (Figure 8 C).

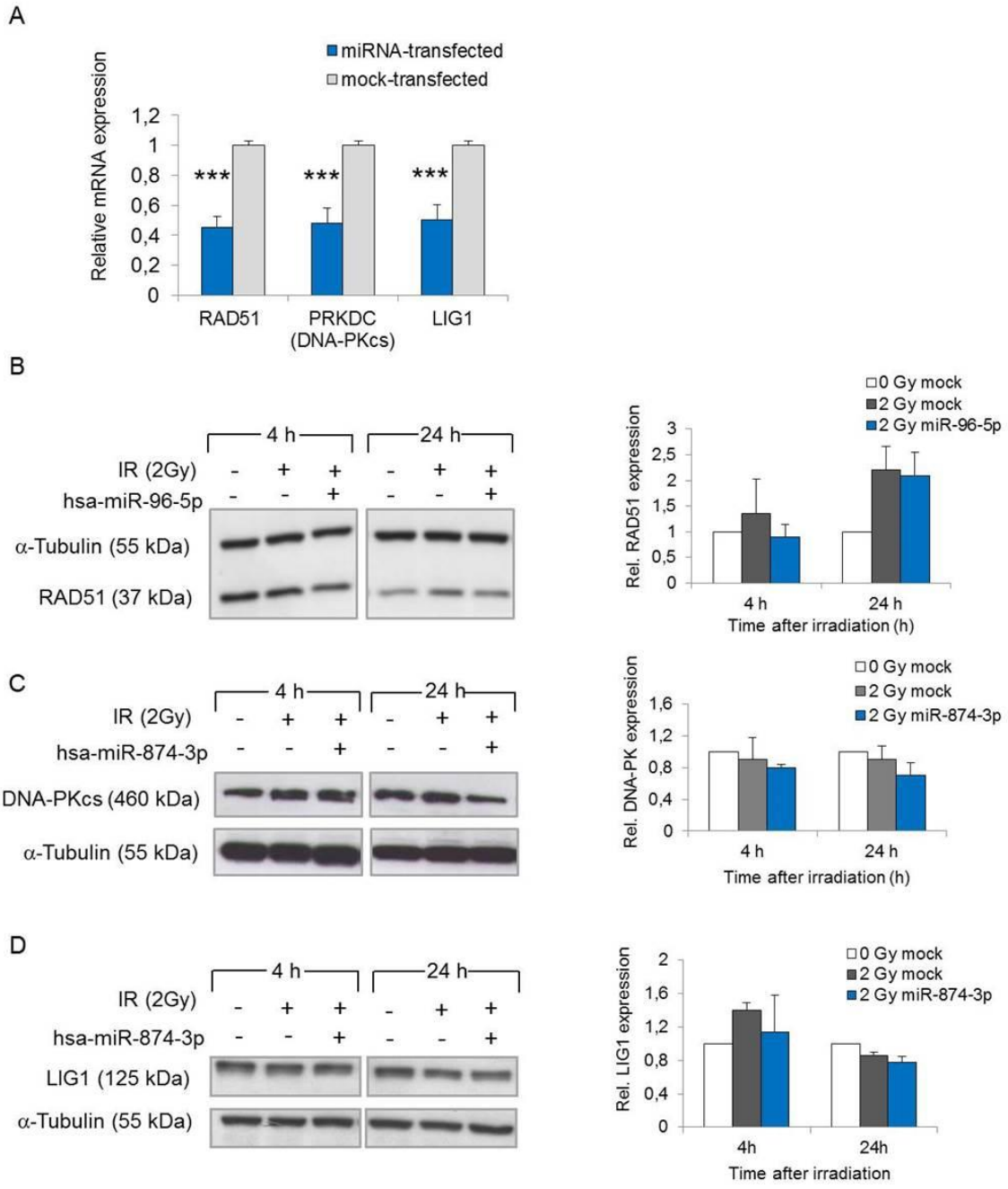

Figure 8. Biological validation of miRNA-mRNA interactions. Analysis of mRNA expression level of RAD51, DNA-PKcs and LIG1 by qRT-PCR in cells transfected 48 h with miRNA mimics irradiated with 2 Gy and recovered immediately after IR (A). The miRNA-treatment decreased significantly the expression level of target genes (***p<0.01). B) Analysis of expression levels of RAD51, DNA-PKcs and LIG1 proteins on whole cell lysates harvested at 4 and 24 h after irradiation. The relative quantification of protein expression levels for each protein (mean ± S.D. of three independent experiments) is shown as fold-change over non-irradiated control cells. C) Western blot analyses on cytosolic and nuclear extraction of proteins harvested at 4 and 24 h after irradiation.

3.4. Effects of miRNA-based treatments on cell survival of irradiated NSCLC A549 cells

To explore the effects of miRNA targeting genes of DSB on radiosensitivity of NSCLC A549 cells we examined the impact of hsa-miR-96-5p and hsa-miR-874-3p overexpression on colony formation ability of 2Gy-irradiated cells. The survival of cells exposed to radiation alone was 51%, which decreased to ~30% when the radiation was combined respectively with the hsa-miR-96-5p and hsa-miR-874-3p mimic (Figure 9 A, p<0.001). When the two miRNAs were used together and combined with radiation no further lowering of survival was observed. The colony counts and plating efficiency of replicate wells between plates were reproducible, generating around the same number of colonies. To evaluate the contribution of HR and NHEJ pathways on cell survival after IR parallel experiments were performed by incubating the cells with specific chemical inhibitors of RAD51 (RI-1), DNA-PKcs (NU7026) and LIG1/LIG3 (L67). The data presented in Figure 9 B show that clonogenic survival was significantly lower for cells treated with inhibitors combined with radiation than cells exposed to radiation alone (RI-1-treated cells: 47.8%; NU7026-treated cells: 41%; L67-treated cells: 49.3%; 2 Gy DMSO: 63.8%). The L67-mediated inhibition of alt-NHEJ pathway was less efficient in reducing cell survival after irradiation, suggesting that this pathway contributed to a lower extent than HR and c-NHEJ to the repair of radio-induced DSBs. Indeed, the combination of RI-1, NU7026, and L67 did not further lower the surviving fraction obtained by RI-1 and NU7026 combination (36%).

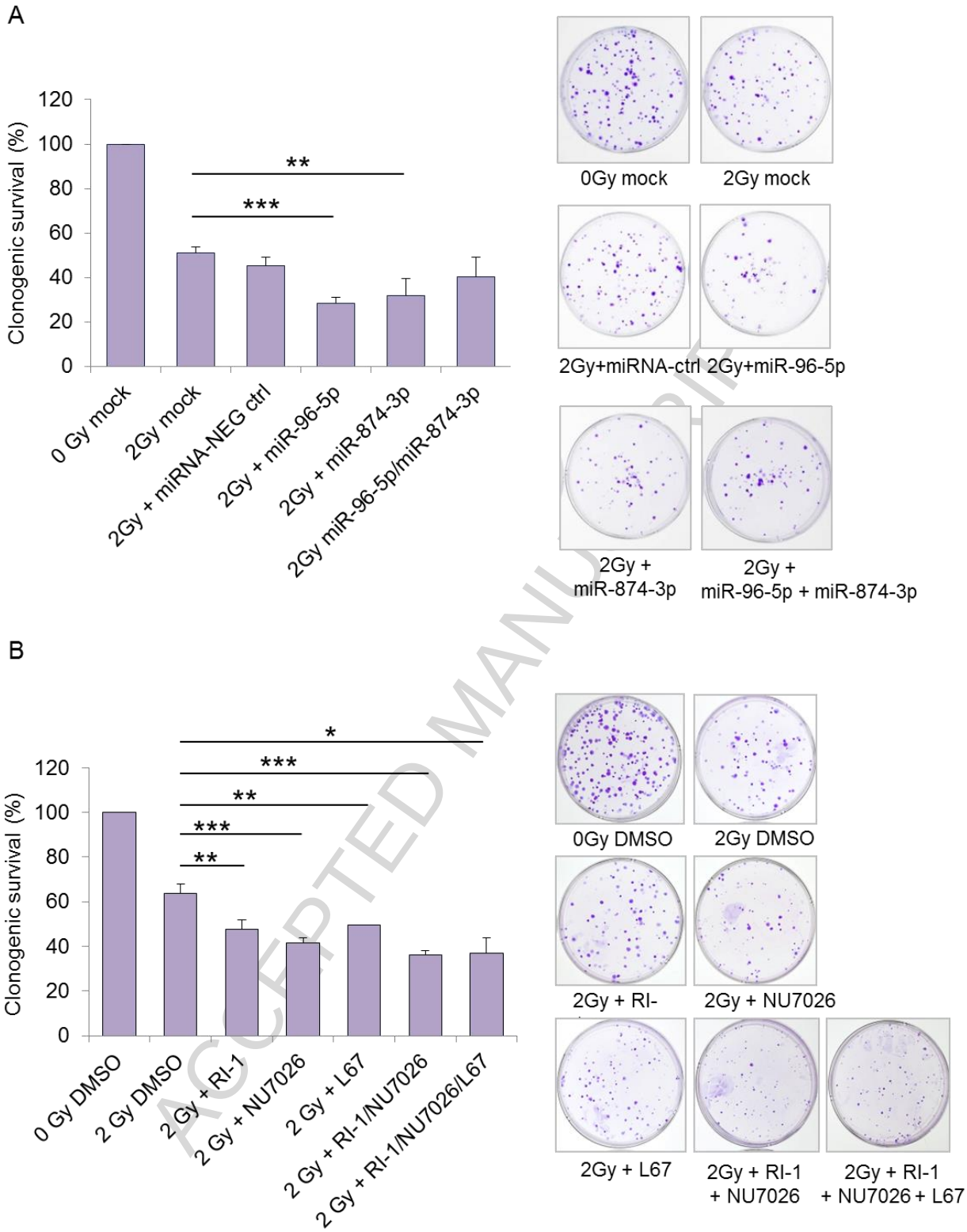

Figure 9. Clonogenic survival of γ-irradiated NSCLC A549 cells treated with miRNA mimics or chemical inhibitors of HR and NHEJ. Before irradiation A549 cells were incubated with miRNA mimics (A) or inhibitors displaying high selectivity for RAD51 (RI-1), DNA-PKcs (NU7026) and LIG1/LIG3 (L67) (B). Cell survival rate was calculated as the percentage of cloning

efficiency of irradiated cells with respect to that of non-irradiated cells. Data refer to means ± S.E. of independent experiments each carried out in quadruplicate ($3 \leq n \leq 10$; ***$p< 0.001$; **$p< 0.01$; *$p<0.05$, *t*-test). Representative images of cell clones derived from miRNA- or inhibitor-based treatments are shown.

The radiosensitizing effect of hsa-miR-96-5p and hsa-miR-874-3p was also tested on NSCLC NCI-H2347 cells (supplementary Figure 3). The results show that clonogenic survival decreased after irradiation in cells transfected with hsa-miR-96-5p but the lowering was not significant compared with mock controls.

3.5. Effects of miRNA-based treatments on DSB repair of irradiated NSCLC A549 cells

We examined the innate DSB repair efficiency of A549 cells by monitoring the appearance and disappearance of γ-H2AX foci as marker of formation and rejoining of DSBs [49]. We quantified the number of γ-H2AX foci at different time points after irradiation (0.5, 2, 6 and 24 h) in cells treated with miRNAs and irradiated with 2 Gy of γ-rays. For comparison, we evaluated the extent of HR and c-NHEJ pathways in the rejoining of IR-induced DSBs when each pathway was chemically inhibited by RI-1 and NU7026 inhibitors, as these two inhibitors mostly affected cell survival compared with L67 (Figure 9). Early after irradiation more than 90% of cells were γ-H2AX foci positive in all conditions, and then the fraction of foci positive cells slightly decreased later after irradiation (Figure 10 A). Approximately 40% of non-irradiated cells displayed endogenous γ-H2AX foci. To better evaluate possible differences of DSB resolution among samples we categorized the cells as having 0-4, 5-9, 10-15 and >15 foci/nucleus. At 0.5 h after irradiation, the fraction of cells retaining >15 foci/nucleus was 2-fold higher in cells overexpressing hsa-miR-96-5p and hsa-miR-874-3p compared with cells treated with radiation alone (~45% vs. 21%, Figure 10 B). At later times the fraction of cells retaining >15 foci/nucleus decreased in hsa-miR-874-3p-treated cells and DSB resolution was complete at 24 h after IR, in contrast to hsa-miR-96-5p-treated cells that retained more foci at 2 and 6 h after irradiation than 2 Gy-mock cells (respectively 30% *vs.* 15% and 20% *vs.* 6%). The presence of RI-1 and NU7026 inhibitors increased respectively the fraction of cells with > 15 foci/nucleus at 0.5 and 2 h after IR, whereas at 6 and 24 h after IR no differences were detected compared with mock-irradiated cells. The fraction of cells with 5-15 foci/nucleus was about 50% at 0.5 h after irradiation, independently from the treatment, and then decreased at later times for all samples except for NU7026-treated cells. In these cells at 24 h after irradiation, the fraction of cells retaining 5-15 foci/nucleus was 2-fold higher than mock-irradiated

cells. The percentage of cells with 0-4 foci/nucleus was low early after irradiation and then increased at later times after irradiation, showing that repair has taken place within the 0.5-24 h time interval (Figure 10 D).

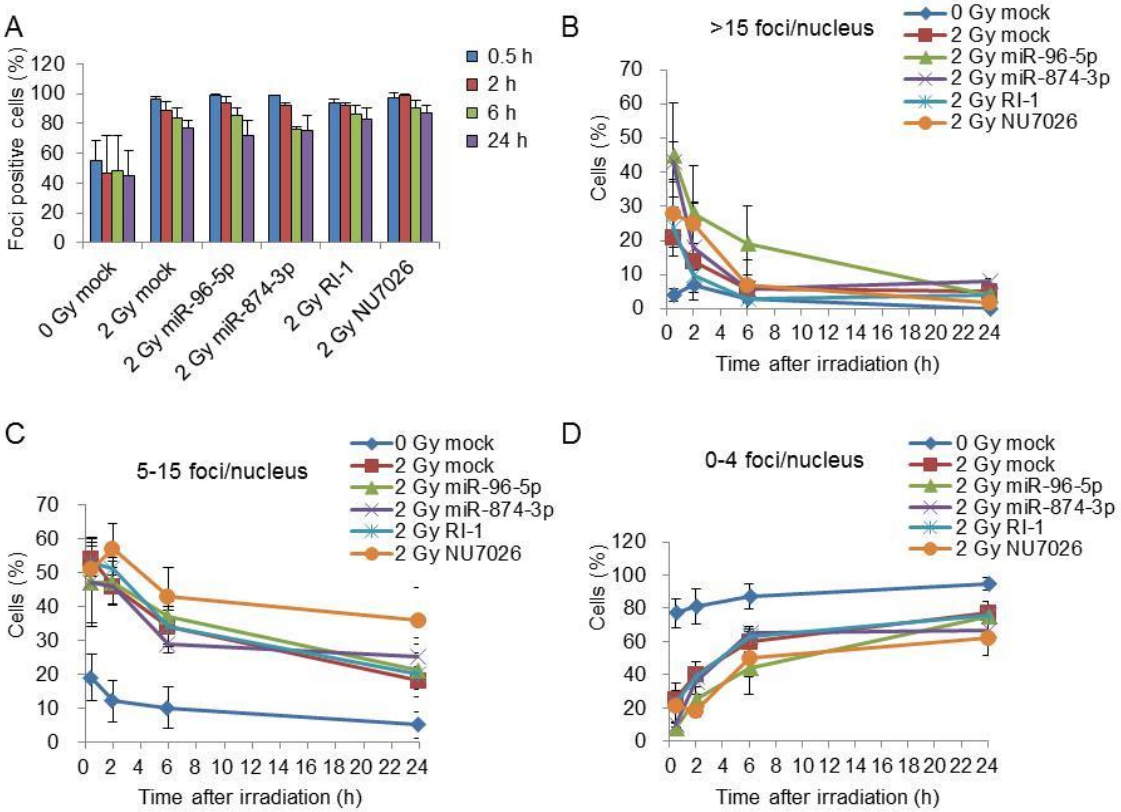

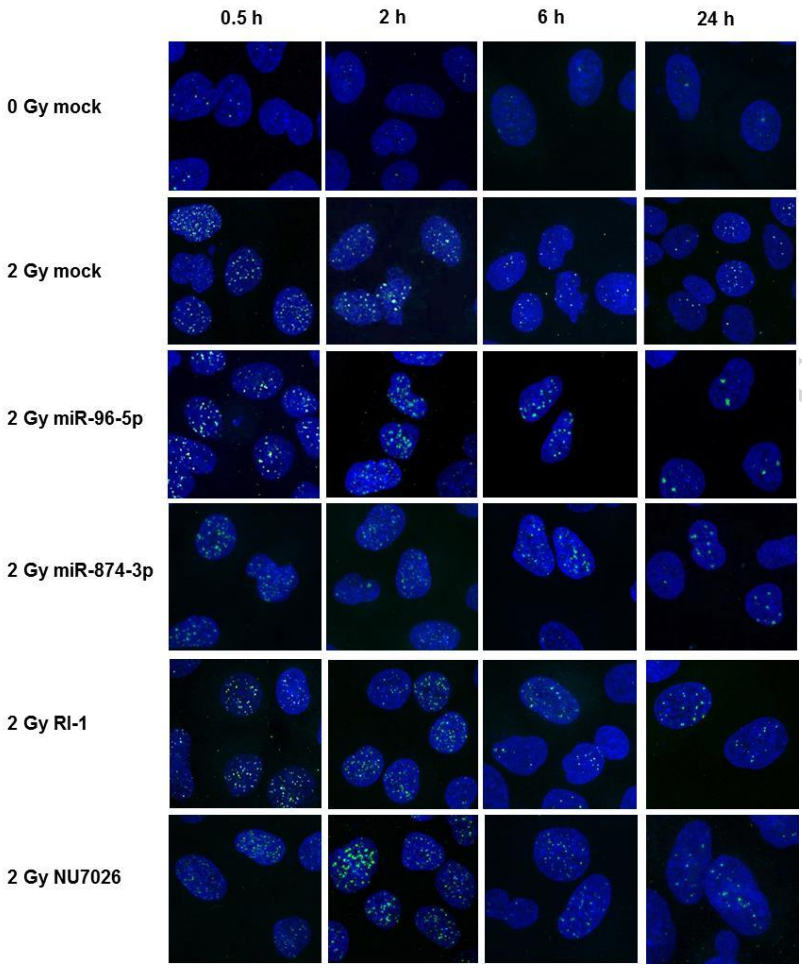

Figure 10. DSB repair efficiency in γ-irradiated cells treated with HR and NHEJ inhibitors or miRNA mimics. Kinetics of the formation and rejoining of radio-induced DSBs was measured by manual counting of γ-H2AX foci at different time points after irradiation. Exponentially growing NSCLC A549 cells were incubated for 48 h with inhibitors or miRNA mimics, irradiated with 2 Gy and then harvested at 0.5, 2, 6, 24 h after irradiation; irradiated and non-irradiated control cells were treated with lipofectamine or DMSO (2 Gy mock; 0 Gy mock). Cells were categorized as having 0-4, 5-15, >15 foci per nucleus. Results are means (± S.D.) of three independent experiments; at least 250-300 cells/time point were scored for foci counting. E) Representative pictures of γ-H2AX foci (green) in nuclei (blue) at 0.5, 2, 6, 24 h after irradiation.

4. Discussion

Radioresistance can occur through efficient repair of DSBs mediated by HR and NHEJ factors. In this regard, the down-regulation of genes involved in such pathways has a potential for increasing radiosensitivity of cells able to escape DNA damage due to a hyperactivity/efficiency of DSB repair. Overexpression of RAD51 is more frequent in cancers than underexpression, as reported in ~30% of *in vivo* NSCLC tumors [50]. Overexpression of DNA-PKcs is found in various cancers, including NSCLC, and closely associated with tumor cell growth, poor prognosis, and clinical therapeutic outcome [51–53]. Higher levels of KU80 protein have been found in lung cancer tissue when compared with normal tissue and associated with lower survival rates [54, 55]. Elevated levels of DNA ligase I have been found in human breast, lung, and ovarian cancer cells versus normal tissues [56] and in neuroblastoma cells [5].

In the current study, we analyzed the miRNA-mediated regulation of DSB genes of HR and NHEJ as a strategy to radiosensitize NSCLC *TP53* wild type cells. A549 cells resulted more tolerant to radiation than NCI-H2347 cells as did not show a dose-dependent G2-phase cell cycle arrest at 24 h after irradiation, even at the highest doses, similarly to radioresistant glioblastoma cells (Figure 1 B-E). Our results are in accordance with Wang et al., [21] that recently classified A549 cells among the nine most radioresistant cells among 58 NSCLC cell lines analyzed for clonogenic survival following irradiation with 2 Gy of γ-rays. Moreover, the colony-formation assay demonstrated that A549 cells are more radioresistant compared with other NSCLC cell lines after exposure to 2-8 Gy doses of irradiation [57]. We thus selected A549 cells for further experiments of miRNA profiling and functional validation studies.

Following genotoxic stress the miRNA response occurs quickly and the most appropriate time points to observe largest changes are dependent on the type of genotoxic stress and cells. We selected two time points after irradiation, 4 and 24 h, frequently analyzed for radiation-induced gene/miRNA expression changes in human cells [26, 41, 58, 59], although largest miRNA responses have been detected in NSCLC cells also at 12 h after irradiation [60]. The results of miRNA expression profiling showed a weak radio responsiveness at both time points after irradiation with 2 Gy, being the value of expression change of differentially expressed miRNAs ± 1.8-fold in irradiated respect to non-irradiated cells (Figure 2). Four differentially expressed miRNAs (hsa-miR-193b-3p, hsa-miR-92a-3p, hsa-miR-21-3p, hsa-miR-6510-5p) were similarly dysregulated in NSCLC A549 cells irradiated with 4-8 Gy of gamma rays [59, 61–62], and four miRNAs (hsa-miR-210-3p, hsa-miR-21-5p, hsa-miR-182-5p, and hsa-miR-126-3p) are reported to be commonly altered in lung adenocarcinoma [43,44,63].

NSCLC A549 cells activated a p53-mediated transcriptional response in response to radiation, as demonstrated by the p53-signalling enhancement, the induction of GADD45A, CDKN1A and

DDB2 transcripts (Figure 4) and the induction of p21 protein at 24 h after irradiation (supplementary Figure 3), according to the *TP53* wild type status of these cells. The overall expression of DSB genes was slightly affected by radiation (Figure 5). The lack of radio responsiveness of these genes is probably related to the high endogenous expression level of the relative transcripts.

The DSB repair genes selected for functional validation in this study are representative of the two essential pathways: HR (*RAD51, BRCA2)* and NHEJ *(PRKDC, XRCC5, LIG1)*. RAD51 and BRCA2 are required for filament formation and strand invasion in HR of double strand breaks, whereas the DNA-dependent protein kinase catalytic subunit (DNA-PKcs) together with KU70 (XRCC6) and KU80 (XRCC5) forms the critical DNA-PK complex essential for NHEJ. The ligase activity of DNA Ligase 1 is required for the ligation of Okasaki fragments during lagging strand DNA synthesis, for the ligation of a newly synthesized patch during base excision repair (BER), and for the final steps of alt-NHEJ that do not rely on microhomologous sequences [8,9]. The critical role of alt-NHEJ has been defined recently in neuroblastoma cells, where the gene silencing of alt-NHEJ components suppresses proliferation, migration, and invasion capacities and the inhibition of Lig1 and Lig3 led to DSB accumulation and cell death [5, 64]. Here, the functional validation studies with luciferase assays demonstrated that *RAD51* is a target of hsa-miR-96-5p, *BRCA2* is a target of hsa-miR-19a-3p, *XRCC5* is a target of hsa-miR-218-5p, and *PRKDC* and *LIG1* are targets of hsa-miR-874-3p (Figure 6). When these miRNAs were over-expressed in NSCLC A549 cells showed a different radiosensitizing potential, therefore validation studies of site-directed mutagenesis were performed on miRNA-mRNA interactions where the miRNA affected clonogenic survival of irradiated cells: hsa-miR-96-5p and hsa-miR-874-3p. As shown in Figure 7 *RAD51*, *PRKDC* and *LIG1* genes are real target of miRNA mimics, as the activity of constructs containing wild type 3'UTR was significantly decreased compared with the mutated 3'UTR.

Hsa-mir-96 is member of the hsa-miR-183-family whose expression is up-regulated in several human cancers comparing cancer with noncancerous tissues [65]. Hsa-miR-96 has been reported to have both oncosuppressor and oncogene functions in different types of cancer, including lung, by promoting or decreasing cell growth [43,66–74]. Several studies have reported tumor suppressive roles of hsa-miR-874, through inhibition of cell cycle and enhanced apoptosis [75–78]. In NSCLC it has been demonstrated that hsa-miR-874 inhibits invasion, migration and cancer stem cell phenotype [45]. Nevertheless, the role of hsa-miR-96-5p and hsa-miR-874-3p in the radiosensitivity of NSCLC has not been elucidated.

The results of *in vivo* biological validation of miRNA-mRNA interactions showed that expression of RAD51 transcript was markedly reduced in cells over-expressing hsa-miR-96-5p, as well as that

of PRKDC and LIG1 transcripts in cells over-expressing hsa-miR-874-3p (Figure 8 A). The expression level of RAD51 protein decreased at both times after irradiation, as observed in whole and fractioned cell lysates (Figure 8 B, E). The expression level of DNA-PKcs protein was affected at 24 h after irradiation in whole cell lysates, and at 4 h after irradiation in the nuclear fraction (Figure 8 D, E). The expression level of LIG1 protein was affected at 24 h after IR in the cytosolic fraction (Figure 8 C, E). On the whole, hsa-miR-96-5p and hsa-miR-874-3p slightly reduced the expression level of RAD51, DNA-PKcs and LIG1 proteins, as could be expected for miRNA targeting constitutive highly expressed proteins [79]. Moreover, the final action of a miRNA on the regulation of protein expression level can vary since endogenous mRNAs often contain many binding sites to different miRNAs [80].

Our results show that over-expression of hsa-miR-96-5p and hsa-miR-874-3p had a great impact on the survival of NSCLC A549 cells after irradiation, by increasing to 20 % their radiosensitivity, similarly to chemical inhibitors of HR and NHEJ repair. The results of chemical inhibition of DSB repair showed that NU7026-treated cells were the most sensitive to IR, indicating that c-NHEJ is the prevailing type of repair to the DSBs radio-induced in A549 cells. The contribution of alt-NHEJ was mild in A549 cells, since approximately 50% of L67-treated cells were still able to form colonies after irradiation with 2 Gy (Figure 9). Moreover, when L67 was combined with RI-1 and NU7026 inhibitors, the survival fraction after irradiation was similar to that of RI-1/NU7026-treated cells (~37 %), without further lowering.

By comparing the results of γ-H2AX foci kinetics we observed that DSB resolution was affected in irradiated cells overexpressing hsa-miR-96-5p, starting from 0.5 h and up to 6 h after irradiation (Figure 10). Cells overexpressing hsa-miR-874-3p showed a higher number of foci at 0.5 h after IR than cells treated with radiation alone but did not show alteration in DSB kinetics within the 24 h interval after IR. Our results suggest that hsa-miR-96-5p and hsa-miR-874-3p can affect DSB repair of NSCLC A549 cells early after irradiation, since at 24 h after irradiation the percentage of γ-H2AX foci-presenting cells decreased to control levels in miRNA-treated cells. The percentage of cells treated with RI-1 and NU7026 inhibitors displaying >15 foci/nucleus was higher at 0.5 and 2 h after IR compared with mock-irradiated cells, whereas at 6 and 24 h after IR no differences were detected. However, at 24 h after irradiation, the fraction of cells retaining 5-15 foci/nucleus was 2-fold higher in NU7026-treated cells than in RI-1- and mock-irradiated cells, indicating the major contribution of NHEJ in the repair of radio-induced DSBs.

Taken together, our results demonstrate the ability of hsa-miR-96-5p and hsa-miR-874-3p to radiosensitize NSCLC A549 cells. These two miRNAs however did not affect significantly the survival of irradiated NCI-H2347 cells (supplementary Figure 3), confirming that the miRNA-

mediated stress response to ionizing radiation is cell type specific. MiRNA mimics have the advantage to carry the same sequence as naturally occurring miRNAs and are, therefore, expected to target the same set of mRNAs that are also regulated by natural miRNAs. However, the miRNA-mediated down-regulation of *RAD51*, *DNA-PKcs* and *LIG1* alone is probably not enough to cause the significant lowering of cell survival of irradiated cells. The final action of hsa-miR-96-5p and hsa-miR-874-3p should consider other target genes in addition to those of DSB repair pathway here validated. However, genes targeted by a single miRNA are commonly related and function in a comparable cellular process, thus the action of a single miRNA can result in a combinatorial effect of gene expression changes in related target genes.

Conclusions

In the current study, we have demonstrated that the combination of miRNA-mediated targeting of *RAD51*, *PRKDC*, *LIG1* genes and IR is effective to enhance cytotoxic effect of therapeutic doses of γ-radiation in NSCLC A549 cells, similarly to specific chemical inhibitors of HR and NHEJ. Sincethe accurate prediction and biological validation of miRNA–target interactions is important to understand the functional role of miRNAs within a tissue-specific cell type, our study can contribute to clarify the role of hsa-miR-96-5p and hsa-miR-874-3p in radioresistant non-small lung adenocarcinoma cells.

Conflict of interests

The authors declare no conflict of interests.

Acknowledgments

This work was supported by the University of Padova (grant number CPDA158287, 2015). We are gratefully to Vito Barbieri (Department of Surgical, Oncological and Gastroenteric Sciences, University of Padova) for cell irradiation. A special thank is for Beniamina Pacchioni (CRIBI, Department of Biology, University of Padova) for technical assistance during microarray experiments and for Cristiano De Pittà (Department of Biology, University of Padova) for data analysis of miRNA profiling. We are gratefully to Umberto Salvagnin (Department of Biology, University of Padova) for photographic support.

References

[1] J.W. Harper, S.J. Elledge, The DNA damage response: ten years after., Mol. Cell. 28 (2007) 739–45. doi:10.1016/j.molcel.2007.11.015.

[2] K. Karanam, R. Kafri, A. Loewer, G. Lahav, Quantitative live cell imaging reveals a gradual shift between DNA repair mechanisms and a maximal use of HR in mid S phase., Mol. Cell. 47 (2012) 320–9. doi:10.1016/j.molcel.2012.05.052.

[3] J. Liu, T. Doty, B. Gibson, W.-D. Heyer, Human BRCA2 protein promotes RAD51 filament formation on RPA-covered single-stranded DNA., Nat. Struct. Mol. Biol. 17 (2010) 1260–2. doi:10.1038/nsmb.1904.

[4] C.A. Waters, N.T. Strande, D.W. Wyatt, J.M. Pryor, D.A. Ramsden, Nonhomologous end joining: A good solution for bad ends, DNA Repair (Amst). 17 (2014) 39–51. doi:10.1016/j.dnarep.2014.02.008.

[5] E.A. Newman, F. Lu, D. Bashllari, L. Wang, A.W. Opipari, V.P. Castle, Alternative NHEJ Pathway Components Are Therapeutic Targets in High-Risk Neuroblastoma., Mol. Cancer Res. 13 (2015) 470–82. doi:10.1158/1541-7786.MCR-14-0337.

[6] G. Lu, J. Duan, S. Shu, X. Wang, L. Gao, J. Guo, Y. Zhang, Ligase I and ligase III mediate the DNA double-strand break ligation in alternative end-joining, Proc. Natl. Acad. Sci. 113 (2016) 1256–1260. doi:10.1073/pnas.1521597113.

[7] L. Deriano, D.B. Roth, Modernizing the nonhomologous end-joining repertoire: alternative and classical NHEJ share the stage., Annu. Rev. Genet. 47 (2013) 433–55. doi:10.1146/annurev-genet-110711-155540.

[8] S. Ahrabi, S. Sarkar, S.X. Pfister, G. Pirovano, G.S. Higgins, A.C.G. Porter, T.C. Humphrey, A role for human homologous recombination factors in suppressing microhomology-mediated end joining., Nucleic Acids Res. 44 (2016) 5743–57. doi:10.1093/nar/gkw326.

[9] A. Decottignies, Alternative end-joining mechanisms: a historical perspective, Front. Genet. 4 (2013) 48. doi:10.3389/fgene.2013.00048.

[10] A. Sfeir, L.S. Symington, Microhomology-Mediated End Joining: A Back-up Survival

Mechanism or Dedicated Pathway?, Trends Biochem. Sci. 40 (2015) 701–714. doi:10.1016/j.tibs.2015.08.006.

[11] A.M. Yu, M. McVey, Synthesis-dependent microhomology-mediated end joining accounts for multiple types of repair junctions., Nucleic Acids Res. 38 (2010) 5706–17. doi:10.1093/nar/gkq379.

[12] J.D. Bradley, R. Paulus, R. Komaki, G. Masters, G. Blumenschein, S. Schild, J. Bogart, C. Hu, K. Forster, A. Magliocco, V. Kavadi, Y.I. Garces, S. Narayan, P. Iyengar, C. Robinson, R.B. Wynn, C. Koprowski, J. Meng, J. Beitler, R. Gaur, W. Curran, H. Choy, Standard-dose versus high-dose conformal radiotherapy with concurrent and consolidation carboplatin plus paclitaxel with or without cetuximab for patients with stage IIIA or IIIB non-small-cell lung cancer (RTOG 0617): a randomised, two-by-two factorial p, Lancet. Oncol. 16 (2015) 187–99. doi:10.1016/S1470-2045(14)71207-0.

[13] B. Movsas, C. Hu, J. Sloan, J. Bradley, R. Komaki, G. Masters, V. Kavadi, S. Narayan, J. Michalski, D.W. Johnson, C. Koprowski, W.J. Curran, Y.I. Garces, R. Gaur, R.B. Wynn, J. Schallenkamp, D.Y. Gelblum, R.M. MacRae, R. Paulus, H. Choy, Quality of Life Analysis of a Radiation Dose-Escalation Study of Patients With Non-Small-Cell Lung Cancer: A Secondary Analysis of the Radiation Therapy Oncology Group 0617 Randomized Clinical Trial., JAMA Oncol. 2 (2016) 359–67. doi:10.1001/jamaoncol.2015.3969.

[14] S. Misra, P. Lal, S. Kumar Ep, N. Rastogi, A. Tiwari, S. Singh, K.J.M. Das, S. Kumar, Comparative assessment of late toxicity in patients of carcinoma cervix treated by radiotherapy versus chemo-radiotherapy - Minimum 5 years follow up., Cancer Treat. Res. Commun. 14 (2018) 30–36. doi:10.1016/j.ctarc.2017.11.007.

[15] A. Aupérin, C. Le Péchoux, E. Rolland, W.J. Curran, K. Furuse, P. Fournel, J. Belderbos, G. Clamon, H.C. Ulutin, R. Paulus, T. Yamanaka, M.-C. Bozonnat, A. Uitterhoeve, X. Wang, L. Stewart, R. Arriagada, S. Burdett, J.-P. Pignon, Meta-Analysis of Concomitant Versus Sequential Radiochemotherapy in Locally Advanced Non–Small-Cell Lung Cancer, J. Clin. Oncol. 28 (2010) 2181–2190. doi:10.1200/JCO.2009.26.2543.

[16] H. Guo, N.T. Ingolia, J.S. Weissman, D.P. Bartel, Mammalian microRNAs predominantly act to decrease target mRNA levels, Nature. 466 (2010) 835–840. doi:10.1038/nature09267.

[17] L. He, X. He, S.W. Lowe, G.J. Hannon, microRNAs join the p53 network--another piece in the tumour-suppression puzzle., Nat. Rev. Cancer. 7 (2007) 819–22. doi:10.1038/nrc2232.

[18] H.I. Suzuki, K. Yamagata, K. Sugimoto, T. Iwamoto, S. Kato, K. Miyazono, Modulation of microRNA processing by p53., Nature. 460 (2009) 529–33. doi:10.1038/nature08199.

[19] U.S. National Institute Of Health, National Cancer Institute. SEER Cancer Statistics Review, 1975–2015. https://seer.cancer.gov/csr/1975_2015/, last visit 2018/10/13.

[20] W. Kim, H. Youn, K.M. Seong, H.J. Yang, Y.J. Yun, T. Kwon, Y.H. Kim, J.Y. Lee, Y.-W. Jin, B. Youn, PIM1-activated PRAS40 regulates radioresistance in non-small cell lung cancer cells through interplay with FOXO3a, 14-3-3 and protein phosphatases., Radiat. Res. 176 (2011) 539–52. http://www.ncbi.nlm.nih.gov/pubmed/21910584.

[21] Y. Wang, J. Gudikote, U. Giri, J. Yan, W. Deng, R. Ye, W. Jiang, N. Li, B.P. Hobbs, J. Wang, S.G. Swisher, J. Fujimoto, I.I. Wistuba, R. Komaki, J. V Heymach, S.H. Lin, RAD50 Expression Is Associated with Poor Clinical Outcomes after Radiotherapy for Resected Non-small Cell Lung Cancer., Clin. Cancer Res. 24 (2018) 341–350. doi:10.1158/1078-0432.CCR-17-1455.

[22] R.M. Phelps, B.E. Johnson, D.C. Ihde, A.F. Gazdar, D.P. Carbone, P.R. McClintock, R.I. Linnoila, M.J. Matthews, P.A. Bunn, D. Carney, J.D. Minna, J.L. Mulshine, NCI-Navy Medical Oncology Branch cell line data base., J. Cell. Biochem. Suppl. 24 (1996) 32–91. http://www.ncbi.nlm.nih.gov/pubmed/8806092.

[23] L.Q. Jia, M. Osada, C. Ishioka, M. Gamo, S. Ikawa, T. Suzuki, H. Shimodaira, T. Niitani, T. Kudo, M. Akiyama, N. Kimura, M. Matsuo, H. Mizusawa, N. Tanaka, H. Koyama, M. Namba, R. Kanamaru, T. Kuroki, Screening the p53 status of human cell lines using a yeast functional assay., Mol. Carcinog. 19 (1997) 243–53. http://www.ncbi.nlm.nih.gov/pubmed/9290701.

[24] S. Toyooka, T. Tsuda, A.F. Gazdar, The TP53 gene, tobacco exposure, and lung cancer., Hum. Mutat. 21 (2003) 229–39. doi:10.1002/humu.10177.

[25] G. Bottai, B. Pasculli, G.A. Calin, L. Santarpia, Targeting the microRNA-regulating DNA damage/repair pathways in cancer., Expert Opin. Biol. Ther. 14 (2014) 1667–83. doi:10.1517/14712598.2014.950650.

[26] C. Girardi, C. De Pittà, S. Casara, G. Sales, G. Lanfranchi, L. Celotti, M. Mognato, Analysis of miRNA and mRNA Expression Profiles Highlights Alterations in Ionizing Radiation Response of Human Lymphocytes under Modeled Microgravity, PLoS One. 7 (2012)

e31293. doi:10.1371/journal.pone.0031293.

[27] H. Wang, R.A. Ach, B. Curry, Direct and sensitive miRNA profiling from low-input total RNA, RNA. 13 (2006) 151–159. doi:10.1261/rna.234507.

[28] B.M. Bolstad, R.A. Irizarry, M. Astrand, T.P. Speed, A comparison of normalization methods for high density oligonucleotide array data based on variance and bias., Bioinformatics. 19 (2003) 185–93. http://www.ncbi.nlm.nih.gov/pubmed/12538238.

[29] A.I. Saeed, N.K. Bhagabati, J.C. Braisted, W. Liang, V. Sharov, E.A. Howe, J. Li, M. Thiagarajan, J.A. White, J. Quackenbush, TM4 microarray software suite., Methods Enzymol. 411 (2006) 134–93. doi:10.1016/S0076-6879(06)11009-5.

[30] K.J. Livak, T.D. Schmittgen, Analysis of relative gene expression data using real-time quantitative PCR and the 2(-Delta Delta C(T)) Method., Methods. 25 (2001) 402–8. doi:10.1006/meth.2001.1262.

[31] B.P. Lewis, C.B. Burge, D.P. Bartel, Conserved seed pairing, often flanked by adenosines, indicates that thousands of human genes are microRNA targets., Cell. 120 (2005) 15–20. doi:10.1016/j.cell.2004.12.035.

[32] V. Agarwal, G.W. Bell, J.-W. Nam, D.P. Bartel, Predicting effective microRNA target sites in mammalian mRNAs, Elife. 4 (2015). doi:10.7554/eLife.05005.

[33] S. Canova, F. Fiorasi, M. Mognato, M. Grifalconi, E. Reddi, A. Russo, L. Celotti, "Modeled microgravity" affects cell response to ionizing radiation and increases genomic damage., Radiat. Res. 163 (2005) 191–9. http://www.ncbi.nlm.nih.gov/pubmed/15658895.

[34] L. Bee, S. Fabris, R. Cherubini, M. Mognato, L. Celotti, The efficiency of homologous recombination and non-homologous end joining systems in repairing double-strand breaks during cell cycle progression., PLoS One. 8 (2013) e69061. doi:10.1371/journal.pone.0069061.

[35] V.G. Tusher, R. Tibshirani, G. Chu, Significance analysis of microarrays applied to the ionizing radiation response., Proc. Natl. Acad. Sci. U. S. A. 98 (2001) 5116–21. doi:10.1073/pnas.091062498.

[36] I.S. Vlachos, K. Zagganas, M.D. Paraskevopoulou, G. Georgakilas, D. Karagkouni, T. Vergoulis, T. Dalamagas, A.G. Hatzigeorgiou, DIANA-miRPath v3.0: deciphering

microRNA function with experimental support, Nucleic Acids Res. 43 (2015) W460–W466. doi:10.1093/nar/gkv403.

[37] M.J. Allalunis-Turner, P.K. Zia, G.M. Barron, R. Mirzayans, R.S. Day, Radiation-induced DNA damage and repair in cells of a radiosensitive human malignant glioma cell line., Radiat. Res. 144 (1995) 288–93. http://www.ncbi.nlm.nih.gov/pubmed/7494872.

[38] S.A. Amundson, K.T. Do, S. Shahab, M. Bittner, P. Meltzer, J. Trent, A.J. Fornace, Identification of potential mRNA biomarkers in peripheral blood lymphocytes for human exposure to ionizing radiation., Radiat. Res. 154 (2000) 342–6. http://www.ncbi.nlm.nih.gov/pubmed/11012342.

[39] M. Mognato, L. Celotti, Modeled microgravity affects cell survival and HPRT mutant frequency, but not the expression of DNA repair genes in human lymphocytes irradiated with ionising radiation., Mutat. Res. 578 (2005) 417–29. doi:10.1016/j.mrfmmm.2005.06.011.

[40] S. Paul, S.A. Amundson, Development of Gene Expression Signatures for Practical Radiation Biodosimetry, Int. J. Radiat. Oncol. 71 (2008) 1236–1244.e76. doi:10.1016/j.ijrobp.2008.03.043.

[41] H.J. Yang, N. Kim, K.M. Seong, H. Youn, B. Youn, Investigation of radiation-induced transcriptome profile of radioresistant non-small cell lung cancer A549 cells using RNA-seq., PLoS One. 8 (2013) e59319. doi:10.1371/journal.pone.0059319.

[42] G. Manning, S. Kabacik, P. Finnon, S. Bouffler, C. Badie, High and low dose responses of transcriptional biomarkers in ex vivo X-irradiated human blood., Int. J. Radiat. Biol. 89 (2013) 512–22. doi:10.3109/09553002.2013.769694.

[43] C. Li, Y. Yin, X. Liu, X. Xi, W. Xue, Y. Qu, Non-small cell lung cancer associated microRNA expression signature: integrated bioinformatics analysis, validation and clinical significance., Oncotarget. 8 (2017) 24564–24578. doi:10.18632/oncotarget.15596.

[44] Z. Peng, L. Pan, Z. Niu, W. Li, X. Dang, L. Wan, R. Zhang, S. Yang, Identification of microRNAs as potential biomarkers for lung adenocarcinoma using integrating genomics analysis, Oncotarget. 8 (2017) 64143–64156. doi:10.18632/oncotarget.19358.

[45] D. Kesanakurti, D.R. Maddirela, S. Chittivelu, J.S. Rao, C. Chetty, Suppression of tumor cell invasiveness and in vivo tumor growth by microRNA-874 in non-small cell lung cancer., Biochem. Biophys. Res. Commun. 434 (2013) 627–33. doi:10.1016/j.bbrc.2013.03.132.

[46] H. Kim, J.M. Yang, Y. Jin, S. Jheon, K. Kim, C.T. Lee, J.-H. Chung, J.H. Paik, MicroRNA expression profiles and clinicopathological implications in lung adenocarcinoma according to EGFR, KRAS, and ALK status, Oncotarget. 8 (2017). doi:10.18632/oncotarget.14298.

[47] X. Xue, X. Fei, W. Hou, Y. Zhang, L. Liu, R. Hu, miR-342-3p suppresses cell proliferation and migration by targeting AGR2 in non-small cell lung cancer, Cancer Lett. 412 (2018) 170–178. doi:10.1016/j.canlet.2017.10.024.

[48] R. Mjelle, S.A. Hegre, P.A. Aas, G. Slupphaug, F. Drabløs, P. Saetrom, H.E. Krokan, Cell cycle regulation of human DNA repair and chromatin remodeling genes., DNA Repair (Amst). 30 (2015) 53–67. doi:10.1016/j.dnarep.2015.03.007.

[49] A. Sharma, K. Singh, A. Almasan, Histone H2AX phosphorylation: a marker for DNA damage., Methods Mol. Biol. 920 (2012) 613–26. doi:10.1007/978-1-61779-998-3_40.

[50] G.-B. Qiao, Y.-L. Wu, X.-N. Yang, W.-Z. Zhong, D. Xie, X.-Y. Guan, D. Fischer, H.-C. Kolberg, S. Kruger, H.-W. Stuerzbecher, High-level expression of Rad51 is an independent prognostic marker of survival in non-small-cell lung cancer patients, Br. J. Cancer. 93 (2005) 137–143. doi:10.1038/sj.bjc.6602665.

[51] C. Beskow, J. Skikuniene, A. Holgersson, B. Nilsson, R. Lewensohn, L. Kanter, K. Viktorsson, Radioresistant cervical cancer shows upregulation of the NHEJ proteins DNA-PKcs, Ku70 and Ku86., Br. J. Cancer. 101 (2009) 816–21. doi:10.1038/sj.bjc.6605201.

[52] H. Hu, Y. Gu, Y. Qian, B. Hu, C. Zhu, G. Wang, J. Li, DNA-PKcs is important for Akt activation and gemcitabine resistance in PANC-1 pancreatic cancer cells., Biochem. Biophys. Res. Commun. 452 (2014) 106–11. doi:10.1016/j.bbrc.2014.08.059.

[53] J. Xing, X. Wu, A.A. Vaporciyan, M.R. Spitz, J. Gu, Prognostic significance of ataxia-telangiectasia mutated, DNA-dependent protein kinase catalytic subunit, and Ku heterodimeric regulatory complex 86-kD subunit expression in patients with nonsmall cell lung cancer, Cancer. 112 (2008) 2756–2764. doi:10.1002/cncr.23533.

[54] J. Ye, Z. Ren, Q. Gu, L. Wang, J. Wang, Ku80 Is Differentially Expressed in Human Lung Carcinomas and Upregulated in Response to Irradiation in Mice, DNA Cell Biol. 30 (2011) 987–994. doi:10.1089/dna.2010.1196.

[55] Z. Zhang, S. Fu, S. Xu, X. Zhou, X. Liu, Y. Xu, J. Zhao, S. Wei, By downregulating Ku80, hsa-miR-526b suppresses non-small cell lung cancer, Oncotarget. 6 (2015) 1462–1477.

doi:10.18632/oncotarget.2808.

[56] D. Sun, R. Urrabaz, M. Nguyen, J. Marty, S. Stringer, E. Cruz, L. Medina-Gundrum, S. Weitman, Elevated expression of DNA ligase I in human cancers, Clin. Cancer Res. 7 (2001) 4143–4148.

[57] W. Ma, C.N. Ma, M. N.N. Zhou, X.D. Li, Y.J. Zhang, Up- regulation of miR-328-3p sensitizes non-small cell lung cancer to radiotherapy, Sci. Rep. 6 (2016) 31651. doi: 10.1038/srep31651.

[58] S. Shin, H.J. Cha, E.M. Lee, S.J. Lee, S.K. Seo, H.O.Jin, I.C. Park, Y.W. Jin, S. An, Alteration of miRNA profiles by ionizing radiation in A549 human non-small cell lung cancer cells, Int J Oncol. 35 (2009) 81–86.

[59] D. Yuan, J. Xu, J. Wang, Y. Pan, J. Fu, Y. Bai, J. Zhang, C. Shao, Extracellular miR-1246 promotes lung cancer cell proliferation and enhances radioresistance by directly targeting DR5, Oncotarget. 7 (2016) 32707–32722. doi:10.18632/oncotarget.9017.

[60] M.T.M. van Jaarsveld, M.D. Wouters, A.W.M. Boersma, M. Smid, W.F.J. van IJcken, R.H.J. Mathijssen, J.H.J. Hoeijmakers, J.W.M. Martens, S. van Laere, E.A.C. Wiemer, J. Pothof, DNA damage responsive microRNAs misexpressed in human cancer modulate therapy sensitivity, Mol. Oncol. 8 (2014) 458–468. doi:10.1016/j.molonc.2013.12.011.

[61] H. Salim, N.S. Akbar, D. Zong, A.H. Vaculova, R. Lewensohn, A. Moshfegh, K. Viktorsson, B. Zhivotovsky, miRNA-214 modulates radiotherapy response of non-small cell lung cancer cells through regulation of p38MAPK, apoptosis and senescence, Br. J. Cancer. 107 (2012) 1361–1373. doi:10.1038/bjc.2012.382.

[62] G. Zhai, G. Li, B. Xu, T. Jia, Y. Sun, J. Zheng, J. Li, miRNA-148b regulates radioresistance in non-small lung cancer cells via regulation of MutL homologue 1, Biosci. Rep. 36 (2016) e00354–e00354. doi:10.1042/BSR20150300.

[63] Q. Zhou, S.-X. Huang, F. Zhang, S.-J. Li, C. Liu, Y.-Y. Xi, L. Wang, X. Wang, Q.-Q. He, C.-C. Sun, D.-J. Li, MicroRNAs: A novel potential biomarker for diagnosis and therapy in patients with non-small cell lung cancer, Cell Prolif. 50 (2017) e12394. doi:10.1111/cpr.12394.

[64] E.A. Newman, S. Chukkapalli, D. Bashllari, T.T. Thomas, R.A. Van Noord, E.R. Lawlor, M.J. Hoenerhoff, A.W. Opipari, V.P. Opipari, Alternative NHEJ pathway proteins as

components of MYCN oncogenic activity in human neural crest stem cell differentiation: implications for neuroblastoma initiation, Cell Death Dis. 8 (2017) 3208. doi:10.1038/s41419-017-0004-9.

[65] Q.-H. Zhang, H.-M. Sun, R.-Z. Zheng, Y.-C. Li, Q. Zhang, P. Cheng, Z.-H. Tang, F. Huang, Meta-analysis of microRNA-183 family expression in human cancer studies comparing cancer tissues with noncancerous tissues, Gene. 527 (2013) 26–32. doi:10.1016/j.gene.2013.06.006.

[66] J. Li, P. Li, T. Chen, G. Gao, X. Chen, Y. Du, R. Zhang, R. Yang, W. Zhao, S. Dun, F. Gao, G. Zhang, Expression of microRNA-96 and its potential functions by targeting FOXO3 in non-small cell lung cancer, Tumor Biol. 36 (2015) 685–692. doi:10.1007/s13277-014-2698-y.

[67] I.K. Guttilla, B.A. White, Coordinate Regulation of FOXO1 by miR-27a, miR-96, and miR-182 in Breast Cancer Cells, J. Biol. Chem. 284 (2009) 23204–23216. doi:10.1074/jbc.M109.031427.

[68] X.M. Xu, J.C. Qian, Z.L. Deng, Z. Cai, T. Tang, P. Wang, K.H. Zhang, J.P. Cai, Expression of miR-21, miR-31, miR-96 and miR-135b is correlated with the clinical parameters of colorectal cancer, Oncol. Lett. 4 (2012) 339–345. doi:10.3892/ol.2012.714.

[69] Y. Shi, Y. Zhao, N. Shao, R. Ye, Y. Lin, N. Zhang, W. Li, Y. Zhang, S. Wang, Overexpression of microRNA-96-5p inhibits autophagy and apoptosis and enhances the proliferation, migration and invasiveness of human breast cancer cells, Oncol. Lett. 13 (2017) 4402–4412. doi:10.3892/ol.2017.6025.

[70] H. Lin, T. Dai, H. Xiong, X. Zhao, X. Chen, C. Yu, J. Li, X. Wang, L. Song, Unregulated miR-96 Induces Cell Proliferation in Human Breast Cancer by Downregulating Transcriptional Factor FOXO3a, PLoS One. 5 (2010) e15797. doi:10.1371/journal.pone.0015797.

[71] Z. Li, Y. Wang, MiR-96 targets SOX6 and promotes proliferation, migration and invasion of hepatocellular carcinoma, Biochem. Cell Biol. (2017) bcb-2017-0183. doi:10.1139/bcb-2017-0183.

[72] S. Yu, Z. Lu, C. Liu, Y. Meng, Y. Ma, W. Zhao, J. Liu, J. Yu, J. Chen, miRNA-96 suppresses KRAS and functions as a tumor suppressor gene in pancreatic cancer., Cancer

Res. 70 (2010) 6015–25. doi:10.1158/0008-5472.CAN-09-4531.

[73] L. Wu, X. Pu, Q. Wang, J. Cao, F. Xu, L.I. Xu, K. Li, miR-96 induces cisplatin chemoresistance in non-small cell lung cancer cells by downregulating SAMD9., Oncol. Lett. 11 (2016) 945–952. doi:10.3892/ol.2015.4000.

[74] H. Guo, Q. Li, W. Li, T. Zheng, S. Zhao, Z. Liu, miR-96 downregulates RECK to promote growth and motility of non-small cell lung cancer cells, Mol. Cell. Biochem. 390 (2014) 155–160. doi:10.1007/s11010-014-1966-x.

[75] B. Zhao, A.-S. Dong, MiR-874 inhibits cell growth and induces apoptosis by targeting STAT3 in human colorectal cancer cells., Eur. Rev. Med. Pharmacol. Sci. 20 (2016) 269–77. http://www.ncbi.nlm.nih.gov/pubmed/26875895.

[76] J. Han, Z. Liu, N. Wang, W. Pan, MicroRNA-874 inhibits growth, induces apoptosis and reverses chemoresistance in colorectal cancer by targeting X-linked inhibitor of apoptosis protein., Oncol. Rep. 36 (2016) 542–50. doi:10.3892/or.2016.4810.

[77] L. Wang, W. Gao, F. Hu, Z. Xu, F. Wang, MicroRNA-874 inhibits cell proliferation and induces apoptosis in human breast cancer by targeting CDK9., FEBS Lett. 588 (2014) 4527–35. doi:10.1016/j.febslet.2014.09.035.

[78] T. Ghosh, A. Varshney, P. Kumar, M. Kaur, V. Kumar, R. Shekhar, R. Devi, P. Priyanka, M.M. Khan, S. Saxena, MicroRNA-874-mediated inhibition of the major G1/S phase cyclin, CCNE1, is lost in osteosarcomas., J. Biol. Chem. 292 (2017) 21264–21281. doi:10.1074/jbc.M117.808287.

[79] J.M. Schmiedel, S.L. Klemm, Y. Zheng, A. Sahay, N. Bluthgen, D.S. Marks, A. van Oudenaarden, MicroRNA control of protein expression noise, Science (80-.). 348 (2015) 128–132. doi:10.1126/science.aaa1738.

[80] A. Krek, D. Grün, M.N. Poy, R. Wolf, L. Rosenberg, E.J. Epstein, P. MacMenamin, I. da Piedade, K.C. Gunsalus, M. Stoffel, N. Rajewsky, Combinatorial microRNA target predictions., Nat. Genet. 37 (2005) 495–500. doi:10.1038/ng1536.

Highlights

1. Gene expression and miRNA profiling in γ-irradiated NSCLC A549 cells
2. Functional validation of miRNA-mRNA interactions involving genes of HR and NHEJ
3. Radiosensitizing effect of hsa-miR-96-5p and hsa-miR-874-3p in NSCLC A549 cells
4. Contribution of HR and NHEJ in the repair of radio-induced DSBs in A549 cells
5. Role of hsa-miR-96-5p and hsa-miR-874-3p in DSB repair of γ-irradiated A549 cells